(2)

TECHNICAL REPORT BRL-TR-3383

BRL

# COMBUSTIBLE CARTRIDGE CASES: CURRENT STATUS AND FUTURE PROSPECTS

F. W. ROBBINS
J. W. COLBURN
C. K. ZOLTANI



AUGUST 1992



U.S. ARMY LABORATORY COMMAND

BALLISTIC RESEARCH LABORATORY
ABERDEEN PROVING GROUND, MARYLAND





## NOTICES

Destroy this report when it is no longer needed. DO NOT return it to the originator.

Additional copies of this report may be obtained from the National Technical Information Service, U.S. Department of Commerce, 5285 Port Royal Road, Springfield, VA 22161.

The findings of this report are not to be construed as an official Department of the Army position, unless so designated by other authorized documents.

The use of trade names or manufacturers' names in this report does not constitute indorsement of any commercial product.

# REPORT DOCUMENTATION PAGE

Form Approved
OMB No. 0704-0188



| 1. AGENCY USE ONLY (Leave blank) | 2. REPORT DATE | 3. REPORT TYPE AND DATES COVERED |
|---|---|---|
| | August 1992 | Final, Oct 91–Apr 92 |

**4. TITLE AND SUBTITLE**
Combustible Cartridge Cases: Current Status and Future Prospects

**5. FUNDING NUMBERS**
PR: 1L162618AH80

**6. AUTHOR(S)**
F. W. Robbins, J. W. Colburn, C. K. Zoltani

**7. PERFORMING ORGANIZATION NAME(S) AND ADDRESS(ES)**

**8. PERFORMING ORGANIZATION REPORT NUMBER**

**9. SPONSORING / MONITORING AGENCY NAME(S) AND ADDRESS(ES)**
U.S. Army Ballistic Research Laboratory
ATTN: SLCBR-DD-T
Aberdeen Proving Ground, MD 21005-5066

**10. SPONSORING / MONITORING AGENCY REPORT NUMBER**
BRL-TR-3383

**11. SUPPLEMENTARY NOTES**

**12a. DISTRIBUTION / AVAILABILITY STATEMENT**
Approved for public release; distribution is unlimited.

**12b. DISTRIBUTION CODE**

**13. ABSTRACT** *(Maximum 200 words)*

The state of the art of our understanding of combustible cartridge cases is presented. The report, after a background section, discusses the models that exist today and presents new models of combustible cartridge case burning. Following a summary of experimental data, it concludes with proposals for further research.

**14. SUBJECT TERMS**
combustible cartridge cases, interior ballistic model, combustion model, closed bomb tests

**15. NUMBER OF PAGES**
67

**16. PRICE CODE**

| 17. SECURITY CLASSIFICATION OF REPORT | 18. SECURITY CLASSIFICATION OF THIS PAGE | 19. SECURITY CLASSIFICATION OF ABSTRACT | 20. LIMITATION OF ABSTRACT |
|---|---|---|---|
| UNCLASSIFIED | UNCLASSIFIED | UNCLASSIFIED | SAR |

INTENTIONALLY LEFT BLANK.

TABLE OF CONTENTS

INTENTIONALLY LEFT BLANK.

## LIST OF FIGURES

INTENTIONALLY LEFT BLANK.

## LIST OF TABLES

INTENTIONALLY LEFT BLANK.

## ACKNOWLEDGMENTS

The authors wish to thank Robert Lieb, U.S. Army Ballistic Research Laboratory (BRL), for furnishing the scanning electron microscope picture. Additional thanks go to Arpad Juhasz, William Aungst, Joyce Newberry, Charles Bullock, and William Oberle, also of BRL, for their work with the design, execution, and analysis of the closed bomb and interrupted burner experiments. We would also like to thank James Bowen, John Hewitt, James Tuerk, William May, Dennis Meyer, and Arthur Koszoru for their help with the gun firings and subsequent data reduction. Lastly, we thank everyone at Armtec Defense Products for communicating their insights into combustible case technology.

INTENTIONALLY LEFT BLANK.

## 1. INTRODUCTION

The use of a cartridge case material which contributes to the energy available to propel a projectile is an intriguing idea and offers a number of advantages. First, the elimination of the metallic cartridge case brings with it a sizeable weight reduction, lessening the demands on the logistics system. Second, the burden, especially on tank gun crews, of disposing of spent cartridges from the crew compartment is reduced to disposing of stub cases. Third, the toxic fumes trapped in the spent metallic cartridges are eliminated. Fourth, for the same volume, more propelling material can be accommodated (volume vs. energy trade-off may lessen or eliminate this advantage).

With these advantages some less desirable properties must be accepted. These include lower mechanical strength than available in metallic cartridge cases, which is important from the packaging point of view; a potential for residue remaining in the barrel after firing, and the concomitant potential for unplanned forward ignition of the next case.

Combustible cartridge cases (CCC) are discussed at some length in Remaly et al. (1974), Brenner and Iqgal (1980), Brabets (1984), Appleman (1986), Puri (1986), Minor and Horst (1986), and Robbins and Colburn (1990). But, even though the CCC has entered the U.S. Army's inventory, some problems with this ammunition type remain. The burning of combustible cases is incompletely understood; thus, performance predictions contain a number of unknowns. Also, there are still some gaps in the experimental database related to combustible cases.

This report, after an introductory section detailing the evolution of CCCs, summarizes both our theoretical understanding and experimental data which is available in Sections 3 and 4, respectively. Section 5 gives an overview of areas needing further research.

## 2. BACKGROUND

2.1 History. CCCs were first developed for the Wehrmacht in World War II. Indeed, even today German industry maintains a sizeable foothold both in the development and the utilization of this technology. It was not until the early 1960s, however, that a combustible case was utilized in a fielded U.S. Army system.

2.2 Types. At the outset, the distinction between consumable and CCCs needs to be made. The former refers to an inert material which is burned as a result of the propellant combustion. A drawback to their use is the need to eliminate residue after a firing. CCCs, on the other hand, contain an oxidizer, usually in the form of nitrocellulose in combination with inert materials, which supplement the energy of the propellant. Here, we distinguish two different types: post impregnated and beater additive.

2.3 Manufacturing Process. The production method of a CCC influences its performance and, consequently, an in-depth look is helpful in understanding its burning characteristics.

Initially, CCCs were manufactured by the impregnation of textiles with resins and oxidizers and the nitration of textiles. However, due to the persistence and presence of residue, the lack of strength of the case, and, most importantly, the sensitivity of ignition, this approach was abandoned. A felting and molding of the inert fibers from fiber slurries was adopted. The die dried molded case also allowed good dimensional tolerance to be maintained.

In the post-impregnation process, the product is impregnated with resins and cured. One drawback is that the concentration of resins is not uniform, which subsequently led to possible uneven burning rates of the case.

In the beater additive approach, which may become the process of choice, the slurry-containing fibrous nitrocellulose and wood fiber has the resin binder added to it. The resins are precipitated onto the fibers before felting, resulting in a more even distribution of the resin throughout the casing. In this process oven curing is eliminated, resulting in a reduction of manufacturing times.

Generally, post-impregnated cases have lower structural strength. But, the most important differences are in the ballistic performance: the different burning mechanisms are reflected in the different pressure curves which result from firings.

## 3. MODELS

The improvement of performance of ballistic components depends on our understanding of the microprocesses taking place during the ballistic cycle. Thus, the underlying purposes of modeling is the characterization of the interior ballistics to conform with experimental observations. One needs to

understand the pressure-time curve, as well as the pressure as a function of distance from the back of the breech to the base of the projectile, the thermodynamic state of the propellants, and the gases generated.

The presence of CCCs complicates the modeling efforts, in that it differs in its combustion characteristics from the propellant, and the CCC is a porous material. From this it follows that the case can be compacted to half of its original thickness at less than the peak maximum gun pressure or about half of its volume is available for gases to penetrate. This brings with it the fact that now there is more free volume available for the propellant gases, thus altering the interior flow behavior.

3.1 Traditional Approaches. Early attempts at predicting the ballistic performance of CCCs were not entirely successful since discrepancies were noted in measured and predicted pressures within the gun chamber. Indeed, when a CCC material was burned in a closed bomb, the apparent burning rate of the CCC material was much higher than would have been found with a gun propellant with the same surface area as the assumed external area of the CCC material. In addition, a size dependence of the burning rate was noted. As we shall see in Section 4.1, disks of cartridge case material burn faster as their size is increased.

To gain more understanding of the CCC material characteristics, the following approach evolved (Figure 1):

(1) Closed-bomb experiments are performed to measure the apparent burning rate of the CCC material. The data is reduced by a burning rate reduction code such as SIMPCB (Juhasz 1982) and incorporated into a burn model.

(2) The burning rate is then used in an interior ballistic code, such as the lumped parameter IBHVG2 or the two-phase NOVA family of codes (XKTC [Gough 1990]), to generate the interior ballistic parameters.

(3) Finally, the performance parameters are compared with actual firing data.

(4) If unacceptable discrepancies are noted, the burn model is modified and the process iterated.

This approach is clearly empirical and post predictive; however, the advantage is that as new data becomes available, it can be readily incorporated into the model. The value of any CCC model will be based on its ability to predict intrinsic burning characteristics accurately.

To answer this challenge, a number of submodels have been developed over the years. Primarily they proceed from the assumption of "additional" burning area being present and its ramification on the burning rates and rate of mass generation.

Two basic models were developed in an attempt to emulate the closed-bomb firing of the CCC. First, it was assumed that the flame had penetrated the entire thickness of the sample and now the individual fibers of nitrocellulose and cellulose or cellulose and binder were then treated as burning as right-circular cylinders. The burning rates for the nitrocellulose were used with the burning characteristics of the cellulose/binder singularly and in combination allowed to vary. The geometry of the fiber material was also varied. As we shall see in Section 3.2, limited success was achieved.

In the second scenario, the model assumed that the flame penetrated a distance into the CCC surface and burned on a given surface area associated with this volume. It was also necessary to fair the flame penetration distance to a constant value over a short time interval. Initial estimates of the internal fiber dimensions and available surface area were based on scanning electric microscope photographs (Figure 2).

One method of modeling the burning CCC characteristics in a gun system is to use the geometry of the CCC in modeling its surface area. The large, single, perforated grain may burn on either the perforation surface or on both surfaces. This surface area is nearly constant. The surface area which would be most like a constant surface area in the closed-bomb firings would be that of the largest sized disks.

Thus, it is assumed that the CCC material burns the same in the gun as in a closed bomb, that it burns only on its inner surface in the 120-mm system, and that static compressibility is the same as during the ballistic cycle. With these assumptions, an approach which will lead to the emulation of the mass generation of the CCC during the ballistic cycle is possible.

To match the gun firing in which there was no CCC using the computer code XKTC (Gough 1990), required a small reduction of the JA2 burning rate. Plots of the ambient experimental pressure time curves and the simulated pressure time curves are given in Figures 3 and 4 and the hot experimental and simulated pressure time curves are in Figures 5 and 6. The pressure gage locations from the rear face of the tube are given on the plots. There is excellent agreement between the simulated curves and the experimental curves. There is a small difference in the time of the uncovering of the pressure gage at position 0 768 m in the hot simulation; this difference is not understood.

After obtaining a match on the no case firing, one would expect to use the apparent burning rates, assuming an $aP^n$ form, of the CCC material from the closed-bomb firings. The burn rate is obtained from the portion in which the apparent burning rates are increasing with pressure (Figure 13). A pressure is chosen at which the burning rates of the CCC material will start to decrease with pressure and a fit with the exponent (it will be negative) from the section of the apparent burning rate curve which is decreasing with pressure is obtained. Next, we iterate on the pressure at which the burn rate of the CCC material starts to decrease until the simulation achieves the correct maximum breech pressure. Finally, we check to see if 50–60% of the case material has burned at the pressure at which the burning of the CCC material starts to decrease. When we did this we found for the post-impregnated case, that iteration on the CCC apparent burning rates from the section where the burning rates are increasing with pressure was not necessary.

The pressure at which the case material burning rate will start to decrease for the post-impregnated CCC was 275 MPa. Modeling the beater additive case gun firings required iterating on the apparent burning rates from the beater additive closed-bomb firings and the pressure at which the case material burning rate will start to decrease. Using the same burning rates for the post-impregnated material in the hot simulation gives reasonable results. The plots of the experimental and simulated pressure time curves are given in Figures 7–12. The specifics of these gun firings are discussed in Section 4.4.

Suggested burning rate equations (pressure in MPa and burning rate in m/s) for 1) post-impregnated case material are:

$$0.002266P^{1.301} \quad < \quad 275 \text{ MPa}$$
$$7.028E7P^{-3} \quad > \quad 275 \text{ MPa;}$$

and, for 2) the beater additive case materials are:

$$0.01598P^{1.479} < 100 \text{ MPa}$$
$$1.4506E5P^{-2} > 100 \text{ MPa.}$$

A simulation with an inert case was also performed to check the compressibility effects. The static measured compressibility which was used in the simulation appears to be reasonable.

Simulations were performed with IBHVG2 version 504 with the equivalent databases used in XKTC. The case was assumed to have been compressed initially by 40% to account for the compressibility effect. The case burns on both the lateral and perforation surface with the case being twice as thick as would be required if the case burned on only one surface. This will emulate burning only on the perforation surface. The chambrage gradient was used to help account for the large amount of chambrage in the 120-mm system. Table 1 contains a comparison of the maximum breech pressure and muzzle velocity for the experimental gun firings and the XKTC and IBHVG2 simulations.

Table 1. Pressure and Velocity Comparisons

| Case Type | Temp (K) | Experimental | | XKTC | | IBHVG2[c] | |
|---|---|---|---|---|---|---|---|
| | | Maximum Breech Pressure (MPa) | Muzzle Velocity (m/s) | Maximum Breech Pressure (MPa) | Muzzle Velocity (m/s) | Maximum Breech Pressure (MPa) | Muzzle Velocity (m/s) |
| none[a] | 294 | 340 | 1,495 | 339 | 1,494 | 338 | 1,474 |
| none[b] | 336 | 430 | 1,582 | 428 | 1,582 | 424 | 1,556 |
| inert | 294 | 364 | 1,524 | 371 | 1,530 | 379 | 1,502 |
| pi[d] | 294 | 474 | 1,626 | 469 | 1,620 | 472 | 1,587 |
| pi[d] | 336 | 576 | 1,694 | 577 | 1,698 | 570 | 1,661 |
| ba[e] | 294 | 490 | 1,639 | 486 | 1,638 | 486 | 1,602 |

[a] Forced to fit - adjusted burning rate (-3%) and barrel resistance
[b] Adjusted burning rate (-2%)
[c] Chambrage gradient option (Robbins et al. 1988)
[d] pi - post-impregnated case
[e] ba - beater additive case

3.2 Fiber Burn Model. The first sub-burn model considered was fiber burn. Here, the matrix making up the propellant is assumed to consist of right-circular cylinders of fibers with L/D ratio of not more than 20. A typical diameter is thought to be between 10 and 40 μm (Figure 2). Since the approximate density of the constituents is known, then the number of fibers of a given diameter and length, which would be contained in a given mass, is calculated. From this follow the maximum surface area available.

The burn model assumes simultaneous ignition of all surfaces of all particles. As a judicious choice of burning rates and initial cylinder dimensions, pressure time curves can be generated which when reduced would yield burning rates in conformance with real burn materials. The problems required unrealistic shapes of the fibers and ad hoc assumptions of the burning characteristics.

A sample run is illustrated in Figure 13 where the length/diameter (L/D) ratio for the nitrocellulose was 1 and diameter 40 μm. The burning rate (in m/s) at 15 MPa was $0.9973 \times 10^{-6} P^{3.0}$; thereafter, between 15 and 20 MPa, it was $0.6629 \times 10^{-3} P^{0.6}$. Between 20 and 115 MPa, it was $0.200 \times 10^{-3} P^{1.0}$ and, finally, between 115 MPa and 300 MPa, it was $0.516 \times 10^{-3} P^{0.8}$. Each of the constituents had its own burning characteristics.

3.3 In-Depth Burning Model. Robbins and Kruczynski (1989) theorized that, in addition to burning taking place on the outside periphery of CCC material, in-depth burning (i.e., burning within the material) might also be present. They suggested modifying the burning model to account for and simulate conditions in which additional surface area, beyond that which is traditionally expected to be involved, becomes available during the burning process.

The mass of propellant burned as a function of time is required in the lumped parameter codes. This information, with the equation of state, is then used to determine the pressure in the chamber and other parameters of interest.

The rate of propellant mass burned, $\dot{m}$ can be expressed as

$$\dot{m} = \rho S \frac{dx}{dt} \quad , \tag{1}$$

where $\rho$ is the density, $S$, the total surface area, and $dx/dt$ the linear burning rate of the propellant. To represent the surface area involved in the volume associated with the in-depth burning, it was postulated that

$$S = S_o + S_e D M \ , \tag{2}$$

where $S$ is the total surface area, $S_o$ the surface area of the grain with burning taking place normal to it, $S_e$ an "effective surface" such that $S_e D$ is the volume in which in-depth burning occurs. Then, $D$ is an "effective" depth to which burning is hypothesized to take place and usually taken as a constant. Finally, $M$, also a constant, is the surface area per unit volume such that $S_e DM$ is the extra surface on which burning takes place in the in-depth volume.

For a single, perforated monolithic grain,

$$S_e = S_o\left(\frac{D+2R}{2R}\right) \ , \tag{3}$$

which is obtained by equating the volumes of the affected propellants, i.e.,

$$S_e D = \pi (R+D)^2 \ell - \pi R^2 \ell \ , \tag{4}$$

where $\ell$ is the length of the grain, $D$ is the radial width, and $R$ the inside diameter of the grain.

In the implementation of the model, both a time and threshold condition was imposed before in-depth burning was allowed to commence.

This model allowed several interesting observations to be made:

(1) If the burning rate is kept the same with in-depth burning taking place, for a small increase in surface in the in-depth volume, a large increase in the maximum breech pressure takes place.

(2) The effect of the interaction of the in-depth volume intersecting the outer grain surface results in a drop in mass generation rate because the surface area decreases after intersection with the outer diameter which leads to an event reminiscent of the slivering of multiperforated propellant.

Although a single, versatile model for in-depth burning has been incorporated into a standard lumped parameter interior ballistic code, not much computational experience exists with it at the present time. The concept is promising and, due to the larger number of degrees of freedom, it warrants further study.

If we apply the in-depth burning model associated with a closed bomb, several assumptions had to be made to match the burning rate curves. The maximum depth of penetration (D) was taken to be 1.7 mm and faired into this distance over 0.2 ms after 20 MPa generated by burning only on the surface of the combustible case disk. The surface area of the in-depth volume (S) was taken to be 50,000 $m^2/m^3$ (Figure 14).

These modeling approaches suggest the need for two-phase, multidimensional, time-dependent reactive models. That is, it will be necessary to predict the flamespreading into CCC material as well as the burning characteristics of different materials.

3.3.1 Model A. Remembering that the material making up a CCC consists of up to 50% by volume of pores, it is not unreasonable to hypothesize that the case material can be modeled as a porous solid with gaseous reactants permeating and, indeed, emanating from it.

Taking our cue from the pulverization of coal in fluidized bed combustion (e.g., Chirone, Massimilla, and Salatino [1991]), the first step in the analysis is to hypothesize an internal structure of the solid which, in turn, then yields an estimate of the area involved in the combustion process with or without the solid.

Considerable literature on percolation considers the topological characteristics of the pore space—three models of which need to be considered in modeling the combustible case. Of paramount interest and importance is the connectivity of the structure in that it substantially influences the mass transport that can take place.*

*Percolation theory describes the morphology of random structures and leads to the definition of an accessibility function. This, in turn, can be related to properties of porous media.

Thus, the solid is considered to consist of a network with occupied sites being the reactive material, vacancies representing the void. Capillary networks and random pore models are built up on this basis.

A Bethe lattice, also sometimes referred to as a Cayley tree, completely characterized by a coordination number equal to 3 is one of the simplest to use. We recall that the coordination number is the number of neighbors connected to a given subpart (i.e., for a cubic tessellation, the coordinate number is 6). The advantage of a Bethe lattice is that there are no reconnections (i.e., no closed loops exist which decrease the mass flux).

Alternatively, the space (i.e., the solid) can be thought to be the subdivided into polyhedra, also called Voronoi tessellation. Then a set of points (the material) is placed randomly in space and enclosed by the smallest polygons that can be formed by planes which bisect the lines connecting the point in question and its neighbors.

In such a situation, as shown, for example, by Talmon and Prager (1978), the "accessible" area, $\hat{a}$, defined as

$$\hat{a}_{ij} = \frac{\textit{area of contact between material } i \textit{ and } j}{\textit{volume } V \textit{ of system}} \quad , \tag{5}$$

is given by

$$\hat{a} = 5.82\, c^{1/3} \phi_i \phi_j \, . \tag{6}$$

Here $c$ represents the number of polyhedra per unit volume, $\phi$ the volume fraction, subscripts $i$ and $j$ refer to two different materials.

Analogously, by probabilistic arguments (Mohanty, Ottino, and Davis 1982) it can be shown that space tesselated by identical cubes of length $\ell$ on a side, where $c = \ell^3$ (number of cubes/unit to volume), the area is given by

$$\hat{a} = 6\, c^{1/3} \phi_i \phi_j \, . \tag{7}$$

In general, then the internal area can be represented as

$$\hat{a} = K[\phi(1-\phi)] . \tag{8}$$

Since not all of the internal area may be accessible, usually

$$\hat{a} = \hat{a}^e + \hat{a}^i , \tag{9}$$

where $\hat{a}^e$ is the accessible part.

The accessible porosity of a coordinated network was given by Fisher and Essam (1961) as

$$\phi^A(\phi) = \phi\left(1 - [\phi^R/\phi]^{(2z-2)/(z-2)}\right) , \tag{10}$$

when $\phi^R$ is the root of the equation

$$\phi^R(1-\phi^R)^{z-2} - \phi(1-\phi)^{(z-2)} = 0 , \tag{11}$$

above the initial threshold which for cubic tessellation lies above $\phi_c > 0.32$.

For a porous solid, with total porosity $\phi$ and whose pore connectivity can be simulated by a Bethe network, the accessible internal surface area per unit volume is then given by

$$\hat{a}^e = K\{\phi(1-\phi) - \phi^i(\phi,z)[1 - \phi^i(\phi,z)]\} , \tag{12}$$

$K$ is a constant and $\phi$ is the "isolated" porosity (i.e., cluster which exist in isolation) (Mohanty, Ottino, and Davis 1982).

The important point here then is, that given a lattice, the internal surface area can be obtained. The type of lattice present depends on the manufacturing process of the combustible case, but a microscopic examination can give good guidance.

Once the surface area, $\mathcal{A}^a$, as a function of the porosity $\phi$ is known, the reaction rates as a function of accessible surface area can be evaluated from

$$r = k_o exp(-E_a/\hat{R}T)C \quad , \tag{13}$$

where $r$ is the reaction rate, $k_o$ the pre-exponential factor, $E_a$ the activation energy, $R$ the gas constant, $T$ the temperature, and $C$ the oxidizer molar concentration. It follows from simple coal combustion models that, if the conversion of the fuel is expressed as

$$m = \frac{\phi - \phi_o}{1 - \phi_o} \quad , \tag{14}$$

the gas generation rate can be written as

$$\frac{dm}{dt} = \left[\frac{r}{\rho(1-\phi_o)}\right]^{a\,a} \quad , \tag{15}$$

showing direct dependence of the gas evolution at the accessible area. This information is then passed on to the lumped parameter interior ballistic code to determine the gun performance.

3.3.2 Model B. An alternate approach, though a complementary model of combustible case combustion, can be established by extending percolation models used to study coal combustion.

Picture a solid (the combustible case) subdivided into small cubic cells. Some contain propellant material, others are void; the sum total of all, though, reflect the overall void fraction of the solid.

The combustion process is simulated by randomly depleting the occupied cells within the matrix by using a Monte Carlo method. The method allows several refinements; preference (i.e, the probability of a reaction taking place) can be given to cells located near or even adjacent to void or open surface cells. An exponential dependance going inversely with distance suggests itself. The depleted cell, at the time of encounter, then immediately is turned into a mass of gas equivalent to that of the solid cells.

The surface area liberated can be tracked by cluster counting techniques; thus, the reaction rate is adjustable accordingly. This technique is very flexible and can be easily calibrated with the pressure measurements already available.

An additional aspect of both of the suggested models is that fragmentation of the lattice can also be included. Fragmentation is hypothesized to take place when the critical void fraction is exceeded. For each of the lattices theoretical values are available.

The cell depletion is directly proportional to the mass generation and the generated information is then used, again in a lumped parameter code to gain insight into gun behavior.

An estimate of the available surface area in a porous solid can also be approached from a fractal point of view. Indeed, air filters, whose efficiency depends on the inner surface of the filter material, have been analyzed along these lines (Pfeifer and Avnir 1983). Essentially, the fractal surface can be shown to be given by

$$area = constant\ (volume)^{D/3} \quad ,$$

where $D$ is the factual dimension, usually between 2 and 3, and the constant turns out to be near 6.

Neither the fractal nor the models A or B have been used in a propellent simulation scenario. They hold promise in advancing the state of the art.

## 4. EXPERIMENTAL VERIFICATION

A series of experiments were conducted to quantify several effects considered to be important for an understanding of CCCs. These included closed-bomb tests to determine apparent burning rates of a combustible case sample and interrupted burner tests to get an idea of the breakup of case material while burning. Finally, gun firings were conducted to determine how ballistic parameters were affected by the case type used.

4.1 Closed-Bomb Experiments. The primary aim of the closed-bomb experiment is to determine the apparent burning rates of combustible case samples. Data thus generated is used in the evolution of CCC

burning models. In addition, interrupted burner tests were performed to obtain a qualitative idea of the breakup of the case material during combustion.

As reported by Colburn and Robbins (1990), a series of closed-bomb tests were performed in an effort to obtain apparent burning rate and sample size dependence data for the beater additive (BA) and post-impregnated case materials. A total of 18 closed-bomb tests were made on the beater additive and post-impregnated case types. The loading density of each charge was maintained at 0.25 g/cm$^3$, while the combustible case samples were varied between three different sized discs. The loading density was kept constant so that relationships could be seen between sample size (disc diameter) and apparent burning rate. A representative plot of apparent burning rate vs. pressure for each sample size and case type is presented in Figure 15. Information derived from the closed bomb and pressure time data is given in Table 2.

The beater additive material showed significantly higher apparent burning rates than similarly sized post-impregnated case material. Since the energy content of the two case types is nearly identical, it was presumed that the difference in resin distribution affected the apparent burning rate of the combustible case material. The magnitudes of the apparent burning rates and the differences in burning rate associated with sample size lead us to believe that the burning mechanism for combustible case materials is something other than would be expected for a nitrocellulose-based propellant of similar shape and size.

Analysis and form function techniques more complex than the initial assumption of simple, uniform density, discs are necessary to model the burning mechanism of combustible case discs in the closed-bomb environment.

4.2 Interrupted Burner Experiments. A series of interrupted burner tests were conducted on the beater additive and post-impregnated case materials to gain a qualitative understanding of how the two case materials burn in a gun environment. A total of 11 tests were conducted with the 2 types of case material. For each run, the chamber was lined with a cylinder of case material, then filled with approximately 72 g of JA2, 7-perforation, granular propellant (Figure 16). The JA2 was stacked in the chamber in an axisymmetric manner. The charge was then initiated with a black powder ignition charge. Charge masses, burst pressures, and comments are shown in Table 3.

Table 2. Three Different Sized Disks at the Same Loading Density in a Closed Bomb

| POST IMPREGNATED | | | | | | | | | |
|---|---|---|---|---|---|---|---|---|---|
| Diameter | 1.11 cm | | | 3.49 cm | | | 6.19 cm | | |
| Maximum Pressure (MPa) | 181 | 220 | 215 | 188 | 189 | 188 | 188 | 190 | 192 |
| Time (ms) 10–90% (Pmax) | 4.31 | 4.12 | 4.20 | 3.63 | 3.58 | 3.48 | 3.50 | 3.65 | 3.41 |
| Maximum dp/dt (MPa/ms) | 64.1 | 71.2 | 77.8 | 79.7 | 80.3 | 79.7 | 88.1 | 92.8 | 115 |
| Pressure (MPa) at Maximum dp/dt | 92.4 | 116 | 112 | 104 | 104 | 107 | 106 | 107 | 115 |
| Initial Surface Area ($m^2$)[a] | .202 | .202 | .202 | .156 | .157 | .157 | .153 | .153 | .154 |
| BEATEK ADDITIVE | | | | | | | | | |
| Diameter | 1.11 cm | | | 3.8 cm | | | 6.35 cm | | |
| Maximum Pressure (MPa) | 201 | 200 | 200 | 205 | 206 | 201 | 208 | 209 | 208 |
| Time (ms) 10–90% (Pmax) | 1.41 | 1.43 | 1.39 | 1.23 | 1.27 | 1.22 | 0.980 | 0.924 | 0.973 |
| Maximum dp/dt (MPa/ms) | 220 | 237 | 241 | 281 | 263 | 276 | 346 | 380 | 353 |
| Pressure (MPa) at maximum dp/dt | 105 | 97.6 | 100 | 103 | 104 | 104 | 104 | 103 | 104 |
| Initial Surface Area ($m^2$)[b] | .219 | .219 | .220 | .155 | .160 | .157 | .151 | .148 | .148 |

[a] assumes density .83 $g/cm^3$ and thickness .00330 m

[b] assumes density .78 $g/cm^3$ and thickness .00348 m

Table 3. Interrupted Burner Data

| Case Type | Case Mass (g) | JA2 Mass (g) | Designed Burst Pressure (MPa) | Maximum Pressure (MPa) | Comments on Recovered CCC Residue |
|---|---|---|---|---|---|
| post impreg. | 26.0940 | 71.3820 | 34.5 | >44.8 | many CCC slivers |
| beater add. | 24.7624 | 71.8184 | 34.5 | >68.9 | CCC "fuzz" |
| post impreg. | 29.0720 | 71.9142 | 6.9 | 17.2 | no residue |
| beater add. | 26.3393 | 72.1131 | 6.9 | 17.2 | large CCC chunks |
| post impreg. | 27.1764 | 72.1866 | 34.5 | 55.2 | many CCC slivers |
| beater add. | 25.7230 | 71.8104 | 34.5 | >68.9 | large CCC chunks |
| post impreg. | 27.4016 | 71.9783 | 68.9 | 68.9 | many CCC slivers |
| beater add. | 25.8464 | 71.4461 | 68.9 | 89.6 | large CCC chunk |
| post impreg. | 28.3219 | 71.9595 | 34.5 | 58.6 | some CCC slivers |
| beater add. | 25.9096 | 71.5074 | 34.5 | 62.1 | lg and sm CCC chunks |
| post impreg. | 29.1016 | 72.1278 | 34.5 | 56.5 | many CCC slivers |
| none | 0.0 | 77.6745 | 34.5 | 48.3 | N/A |
| none | 0.0 | 77.3005 | 34.5 | 48.3 | N/A |

In general, the interrupted burner technique was not very effective with CCC material because the case material that had not been consumed before the burst disc ruptured continued to burn or smolder after disc rupture. This limited sample recovery to only the larger case pieces which were manually extinguished before they were completely consumed.

The recovered case pieces were quite interesting. The post-impregnated case pieces consisted exclusively of material from the high-resin density layer which was adjacent to the chamber wall. The high-resin density layer adjacent to the propellant and the inner low-resin density region had burned away completely.

The recovered beater additive case pieces showed mechanical damage and, in some cases, charring from post-burst burning. However, all pieces appeared to be nearly the full thickness of the pretest

samples. This indicated that the beater additive case sections which were ignited burned away completely, while the unignited portions, which were probably farther from the ignition charge and closer to the burst disc, were not involved in combustion before the disc ruptured. The results indicated that the beater additive case burned more uniformly than the post-impregnated case, presumably because of the more uniform resin density in the beater additive case samples.

An ancillary data set was reported by Robbins, Koszoru, and Minor (1986). One of the significant findings of their study was that a CCC can be compressed to half its original thickness at less than maximum gun pressure, yielding an increase in the free volume available to the propellant gases (i.e., larger ullage volume). Closed-bomb testing produced apparent burning rates well above those expected, suggesting that delamination or in-depth burning may occur during combustion.

The closed-bomb burning rates for the combustible case material used was that for 829 case material. The burning rates were very high at moderate pressures (250 mm/s at 70 MPa) and is assumed to capture the delamination or in-depth burning process. The burning rate equation used was $r = 1.03 \cdot P^{1.301}$ where again $P$ is in MPa and $r$ is in mm/s. Based on the gun firings discussed in the next section, a model incorporating compressibility and adjusted buring rate evolved. The results are shown in Figure 17 where experimental data are compared in the prediction from XKTC (Gough 1990).

Compressibilities for both the inert case material and the combustible case material from a DM13 cartridge were measured at low loading rates. The resulting compressibility data is given in Table 4. The initial thicknesses of the kraft and combustible cases were 3.30 mm and 3.68 mm, respectively.

Table 4. Compressibility of Cartridge Case Material

| Kraft Case | | Combustible Case | |
|---|---|---|---|
| Pressure (MPa) | Density ($g/cm^3$) | Pressure (MPa) | Density ($g/cm^3$) |
| 0.101 | 0.656 | 0.101 | 0.817 |
| 48.3 | 1.032 | 75.9 | 1.259 |
| 145.0 | 1.207 | 172.0 | 1.376 |
| 690.0 | 1.329 | 690.0 | 1.517 |

The increase in maximum breech pressure (> 100 MPa) of the combustible case over the inert case gun firings demonstrates the large influence of the combustible case. The XKTC (Gough 1990) calculations, as well as closed-bomb results, indicate that the combustible case does not burn in a linear manner but breaks up and/or delaminates or burns in-depth, providing a significant increase in surface area early in the ballistic cycle.

4.3 Initial Gun Firings. Gun firings seek to determine what effects the various case material type have on macroscopic ballistic parameters. In addition, they gauge the validity of the computer model in use. A series of gun firings was also reported by Robbins, Koszoru, and Minor (1986) using a conventional DM13 kinetic energy round. Firings were performed in a 120-mm gun.

In order to experimentally assess the interior ballistic significance of these attributes of the combustible case, a series of firings with a conventional kinetic energy round employing a combustible case was conducted. The German 120-mm, kinetic energy DM13 cartridge was selected because of its ready availability and large firing database. The procedure followed was to fire the DM13 cartridges with no case, cartridges with inert cases, and finally, cartridges with combustible cases. The gun firings without any case should allow the characterization of the barrel resistive profile (the pressure which must be overcome just to have projectile motion as a function of distance the projectile travels down the tube), assuming the measured burning rates of the 7-perforated JA2 propellant are correct. The firings with the noncombustible case should yield the effect of the volume of the case, and, if required, the effects of case compressibility (under the assumption the inert case does not burn significantly during the ballistic cycle). Finally, gun firings with the combustible case should yield the combustion characteristics of the combustible case.

The gun firings were performed at the U.S. Army Ballistic Research Laboratory's Sandy Point Test Facility (R-18) on June 12, 1985. The 120-mm gun system used included an XM256 tube and an XM256 breech in an Aberdeen Proving Ground sleigh using a M158 recoil system. The tube was instrumented with five pressure gages in the chamber: two at 95 mm, one at 286 mm (midchamber), and two at 489 mm from the rear face of the tube. There were also seven gages down-bore at 768 mm, 1,048 mm, 1,530 mm, 2,292 mm, 3,054 mm, 3,816 mm, and 4,578 mm from the rear face of the tube. The pressure gages used were Kistler Model 6211's. All the cases were drilled to allow free access of the combustion gases to the pressure gages in the chamber. The entire matrix of firings was done on the same day with the same pressure gages. All charges were conditioned to 21° C.

Velocity measurements were attempted using a HYCAM 16-mm camera at 3,000 frames per second. The position of the projectile was difficult to determine from the films, leading to a large scatter in velocities for the same condition, thus rendering the data unusable.

After a DM13 cartridge was fired as a warmer and checkout round, the charges were fired in sets of four with the DM13 cartridge fired first, a caseless round, a round with the M827 case, and the inert case round last. These sets of firings were repeated 3 times for a total of 12 rounds. The maximum breech pressures recorded by the two gages at 95 mm from the rear face of the tube are tabulated in Table 5.

Table 5. Experimental Maximum Breech Pressures

| Round | DM13 (MPa) | Round | Caseless (MPa) | Round | M827 Case (MPa) | Round | Inert Case (MPa) |
|---|---|---|---|---|---|---|---|
| 1 | 510 | 2 | 383 | 3 | 505 | 4 | 380 |
| | 512 | | 384 | | 502 | | 385 |
| 5 | 501 | 6 | 380 | 7 | 500 | 8 | 388 |
| | 497 | | 380 | | 497 | | 386 |
| 9 | 505 | 10 | 382 | 11 | 510 | 12 | 392 |
| | 502 | | 381 | | 506 | | 389 |
| average | 502 | | 382 | | 503 | | 387 |
| (std. dev.) | (5.68) | | (1.63) | | (4.63) | | (4.08) |

4.4 Additional Gun Firings. The gun was instrumented with 13 Kistler Model 6211 pressure gages. Velocities were measured with a 10.5-GHz WEIBEL down-range Doppler radar system, and with a pair of WEIBEL Sky Screens centered 36 m from the muzzle. Data were taken on the PDP11-45 based BALDAS system, and on the HP9020/Multitrap-based Telemetry Acquisition Reduction and Plotting System (TARPS) data acquisition system. The firing matrix along with the round identifier codes for the test rounds is shown in Table 6. Peak pressure data are shown in Table 7 and velocity data are shown in Table 8.

The gun firings were designed to quantify the effects of different cartridge cases on measurable ballistic parameters. A series of 19 test rounds were fired to compare the characteristics of the different cartridge case types, and to establish a database for comparison with computer models. The test rounds were based on the German 120-mm DM13, APFSDS round, shown in line diagram form as Figure 18.

Table 6. DM13 Firing Matrix

| Round Identifiers | Case Type | No. of Rounds | Conditioning Temperature (°C) |
|---|---|---|---|
| PI 1 and PI 2 | post-impregnated | 2 | 21 |
| PI 3 and PI 4 | post-impregnated | 2 | 63 |
| BA 1 and BA 2 | beater additive | 2 | 21 |
| I 1 and I 2 | inert | 2 | 21 |
| NC 1 and NC 2 | no case | 2 | 21 |
| NC 3 and NC 4 | no case | 2 | 63 |

Table 7. DM13 Firing Data, Pressure Peaks

| | Displacements From Breech (cm) | | | | | | | | | | |
|---|---|---|---|---|---|---|---|---|---|---|---|
| ID | 9.5 | 28.6 | 48.9 | 76.8 | 104.8 | 153.0 | 229.2 | 305.4 | 381.6 | 457.8 | 534.0 |
| I1 | 366 | 370 | 346 | 303 | 289 | 249 | 206 | 173 | 129 | 97 | 75 |
| I2 | 362 | 367 | 342 | 302 | 287 | 252 | 193 | 170 | 125 | 92 | 71 |
| NC1 | 340 | 347 | 328 | 283 | 272 | 240 | 201 | 161 | 131 | 95 | 66 |
| NC2 | 341 | 348 | 330 | 278 | 281 | 241 | 187 | 172 | 125 | 96 | 74 |
| NC3 | 432 | 430 | 419 | 348 | 348 | 287 | 232 | 155 | 103 | 79 | 59 |
| NC4 | 428 | 428 | 416 | 346 | 348 | — | 224 | 160 | 108 | 79 | 59 |
| PI1 | 478 | 479 | 462 | 373 | 342 | 296 | 217 | 166 | 124 | 85 | 62 |
| PI2 | 471 | 463 | 445 | 373 | 350 | 311 | 219 | 162 | — | 83 | 61 |
| PI3 | 569 | 557 | 536 | 539 | 433 | 379 | 232 | 155 | 104 | 79 | 50 |
| PI4 | 583 | 570 | 550 | 454 | 432 | 335 | 233 | 158 | 106 | 82 | 47 |
| BA1 | 486 | 488 | 456 | 382 | 345 | 290 | 228 | 173 | 117 | 82 | 56 |
| BA2 | 494 | 482 | 464 | 380 | 349 | 286 | 215 | 166 | 116 | 84 | 61 |

Table 8. DM13 Firing Data, Velocities

| Round ID | Doppler Muzzle Velocity (m/s) | Doppler Velocity at 36 m (m/s) | Sky Screen Velocity at 36 m (m/s) |
|---|---|---|---|
| I1 | 1,523 | — | 1,521 |
| I2 | 1,524 | 1,523 | 1,523 |
| NC1 | 1,495 | — | 1,493 |
| NC2 | 1,495 | 1,493 | 1,494 |
| NC3 | 1,582 | 1,580 | — |
| NC4 | 1,583 | 1,581 | 1,587 |
| PI1 | 1,624 | 1,623 | 1,625 |
| PI2 | 1,628 | 1,624 | 1,623 |
| PI3 | 1,688 | 1,686 | 1,692 |
| PI4 | 1,699 | 1,697 | 1,705 |
| BA1 | 1,639 | 1,636 | -42 |
| BA2 | 1,639 | 1,636 | 1,636 |

This round was chosen because of its relatively high availability, and because it had well-documented performance characteristics. A nominal DM13 consisted of a post-impregnated CCC, a bayonet primer, a projectile/sabot assembly, and a nominal 7.32 kg of 7-perforated JA2 granular propellant. Seven of the rounds were left unaltered and used as check-out rounds for the data acquisition systems. These rounds were expected to give performance similar to that of the rounds equipped with a post-impregnated case. The other 12 rounds were broken down then reassembled as per the matrix shown in Table 6.

The "no-case" rounds formed a baseline database for computer code analysis of the test rounds. By removing the complex combustible case component from the input database, an approximation of the resistive pressure profile of the DM13 round could be formulated and used as a known variable for analysis of subsequent rounds with more complex input databases. These firings were done at both 21° C and 63° C.

The inert case rounds were fired to define the effects of the case's volume and compressibility on the ballistic cycle. The inert case occupies the same volume as a combustible case but it burns very little during the ballistic event. After firing each of the inert case rounds, a significant portion of each inert case was recovered intact. The portions of the case which were missing appeared to have been removed by mechanical means, not consumed by combustion.

The post-impregnated case rounds were fired at both 21° C and 63° C. These rounds provided experimental comparison data for use with the model of the post-impregnated case.

The beater additive case rounds provided data for use with the case modeling effort, and made an interesting comparison between identical rounds equipped with post-impregnated and beater additive cases.

## 5. RESULTS

The significant difference between the apparent burning rates for the post-impregnated and beater additive case materials in the closed-bomb tests indicate that the two case types have different burning characteristics. This may necessitate the use of different form functions, models, or techniques when modeling the cases with interior ballistic codes.

The collected gun firing data provide no new charge performance information, just performance levels to be emulated by interior ballistic computer modeling programs. The specific pressure levels recorded are not of general interest to the ballistic community, but the comparison of those levels can be quite interesting.

As detailed in Table 7, the difference between the average chamber pressures of the inert case and no-case rounds fired at 21° C is 24 MPa. This is the difference expected because of the volume occupied by the inert case. The pressure difference also indicates that the portion of the propellant placed in each bag in the no-case charges more closely approximated the configuration of an unaltered round. This is different from previous work (Robbins, Koszoru, and Minor 1986) where the expected pressure difference was not seen due to excessive ullage in the forward propellant bag.

The other breech pressure difference of interest is that between the beater additive case rounds and the post-impregnated case rounds fired at 21° C. The difference suggests that the significant differences in the apparent burning rates seen in the closed-bomb tests are also seen in the gun firings.

Several approaches to the theoretical modeling of CCC material have been discussed. Clearly, the ground work has been laid, but more computer simulation needs to be performed for a better theoretical understanding of the burning characteristics of combustible cases.

## 6. AREAS FOR FURTHER RESEARCH

Our present understanding of CCC is still rudimentary. This is reflected in the semiempirical models in current use. Much more experimental data is needed before the theoretical models can make progress. Research is needed in the following areas:

(1) Complete closed-bomb studies to evaluate loading density and edge effect.

(2) Edge treated disks of the CCC material need to be studied, especially with regard to the burn rates.

(3) Closed-bomb studies on a variety of CCCs, nitration levels, post-impregnated/beater additive need to be performed.

(4) Gun firings are needed at various charge-to-mass ratios. This should include combinations of projectiles and propellant weights both for the 120- and 155-mm guns.

(5) The effect of ullage on the performance of CCCs needs to be addressed. Do caliber size and initial configurations (i.e., no ullage vs. ullage) affect the burning characteristics?

(6) A visual observation supplemented by state of the art detection of the burning to clarify some issues such as the location of combustion sites within the chamber and in the grain needs to be performed.

(7) In situ computed tomography as well as x-ray cinematography studies under dynamic conditions would shed considerable light on the burning process.

(8) Mercury penetration porosimetry (Androutsopoulos and Mann 1979) or some other technique needs to be used to determine the pore size distribution in the combustible case.

(9) The proposed new models need to be tested against available data.

## 7. CONCLUSIONS

Since their introduction, considerable headway in characterizing CCC behavior has been made. But the picture is still incomplete. Experimental data, especially from gun firings is limited. In addition, our models are still semiempirical and case-specific and only in a limited sense predictive.

In these writers' opinion, the evidence is compelling that some sort of in-depth flame spreading plays an important role in the combustion dynamics of combustible cases. Though not completely understood, at present the relative roles of nitrocellulose and cellulose fiber burning will need to be further elucidated.

Further research is indicated. Suggestions toward these ends have been presented.

Until further research is performed, a sensible approach is to use the relations discussed in Section 3.1 (pages 5 and 6).

## COMBUSTIBLE CASE: MODELS AND BURN SUBMODELS

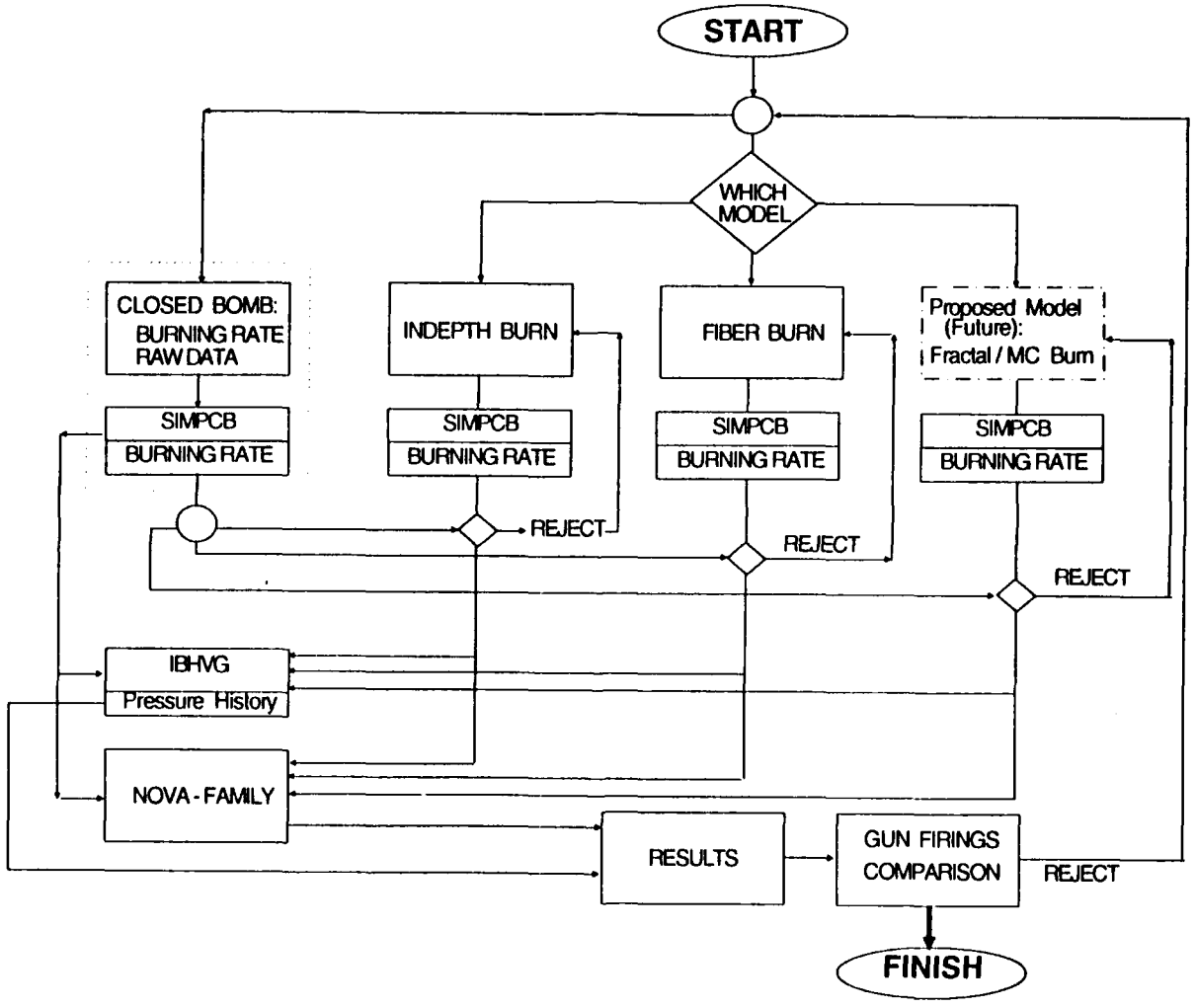


Figure 1. Combustible Case: Models and Burn Submodel.

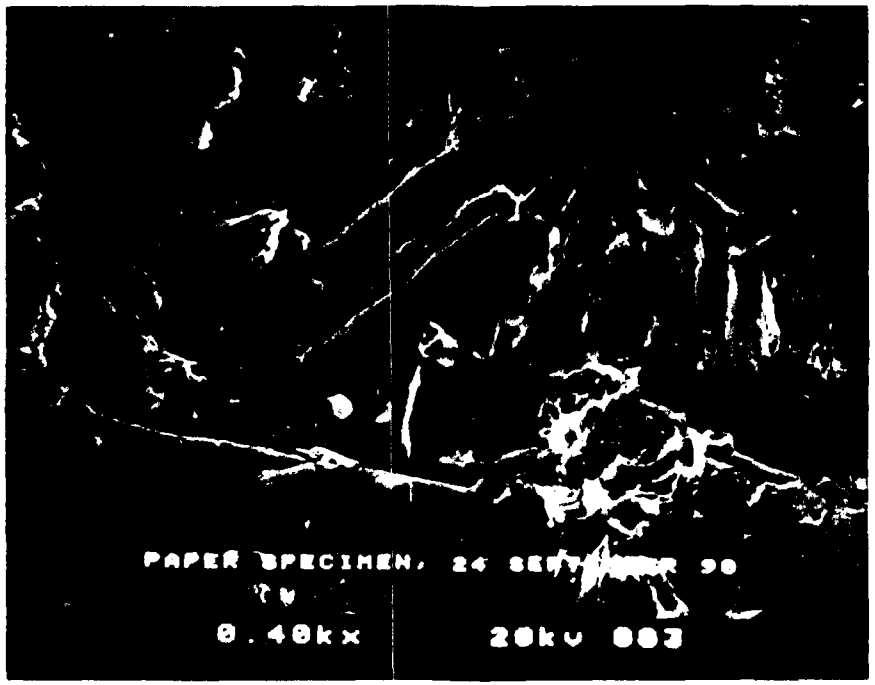


Figure 2. Scanning Electron Microscope Image of a Combustible Case.

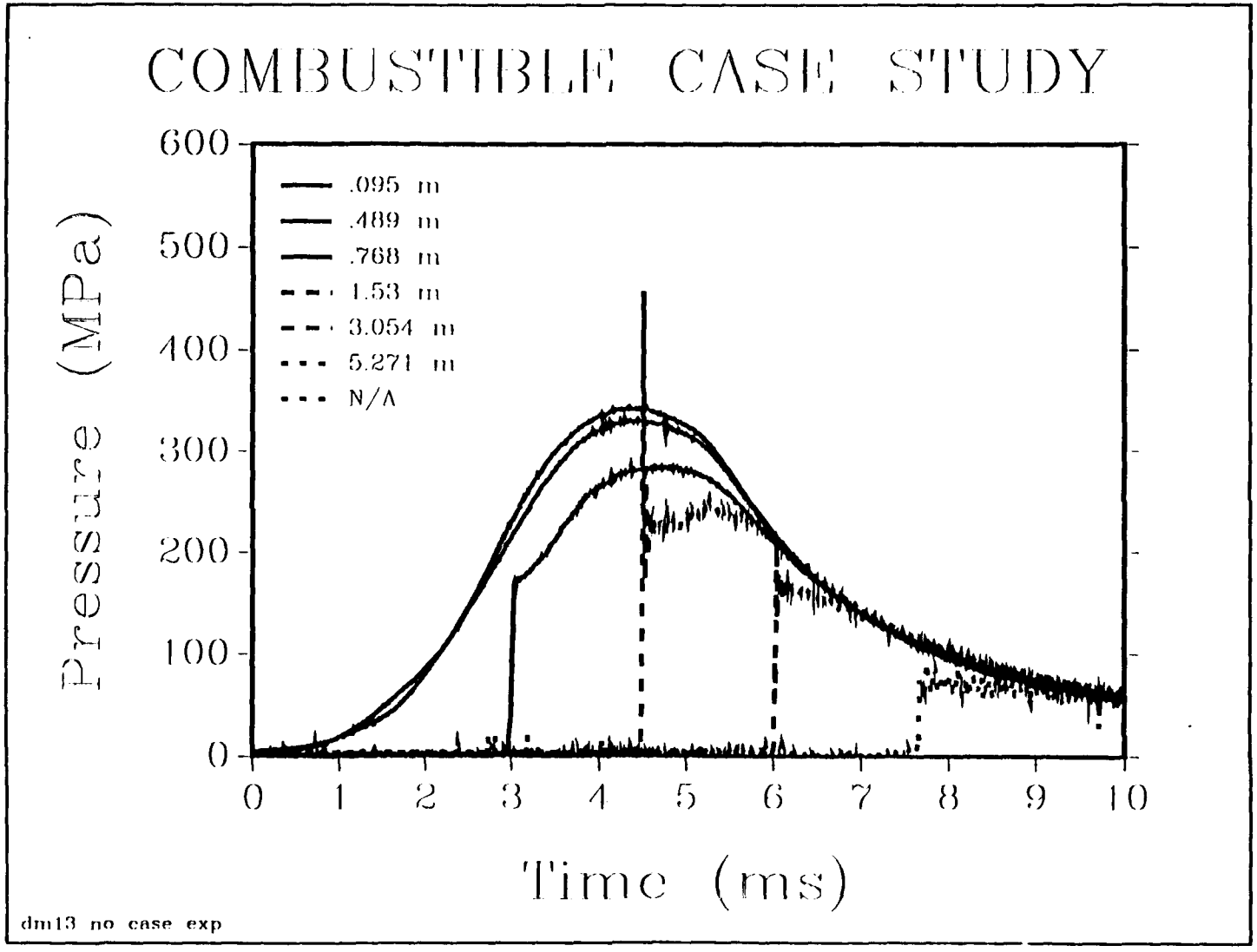


Figure 3. Experimental Pressure Time Curve - No Case - Ambient.

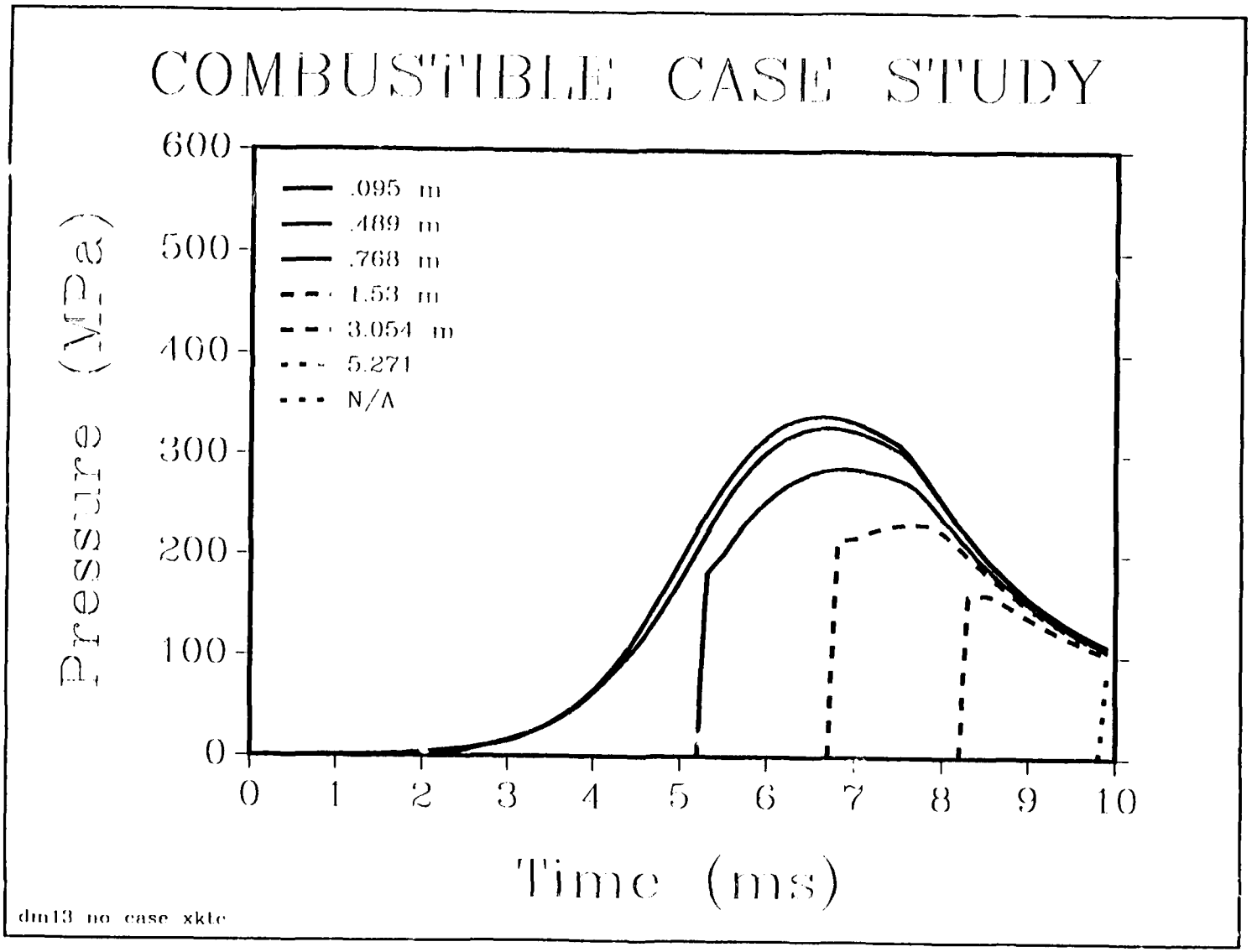


Figure 4. Theoretical Pressure Time Curve - No Case - Ambient.

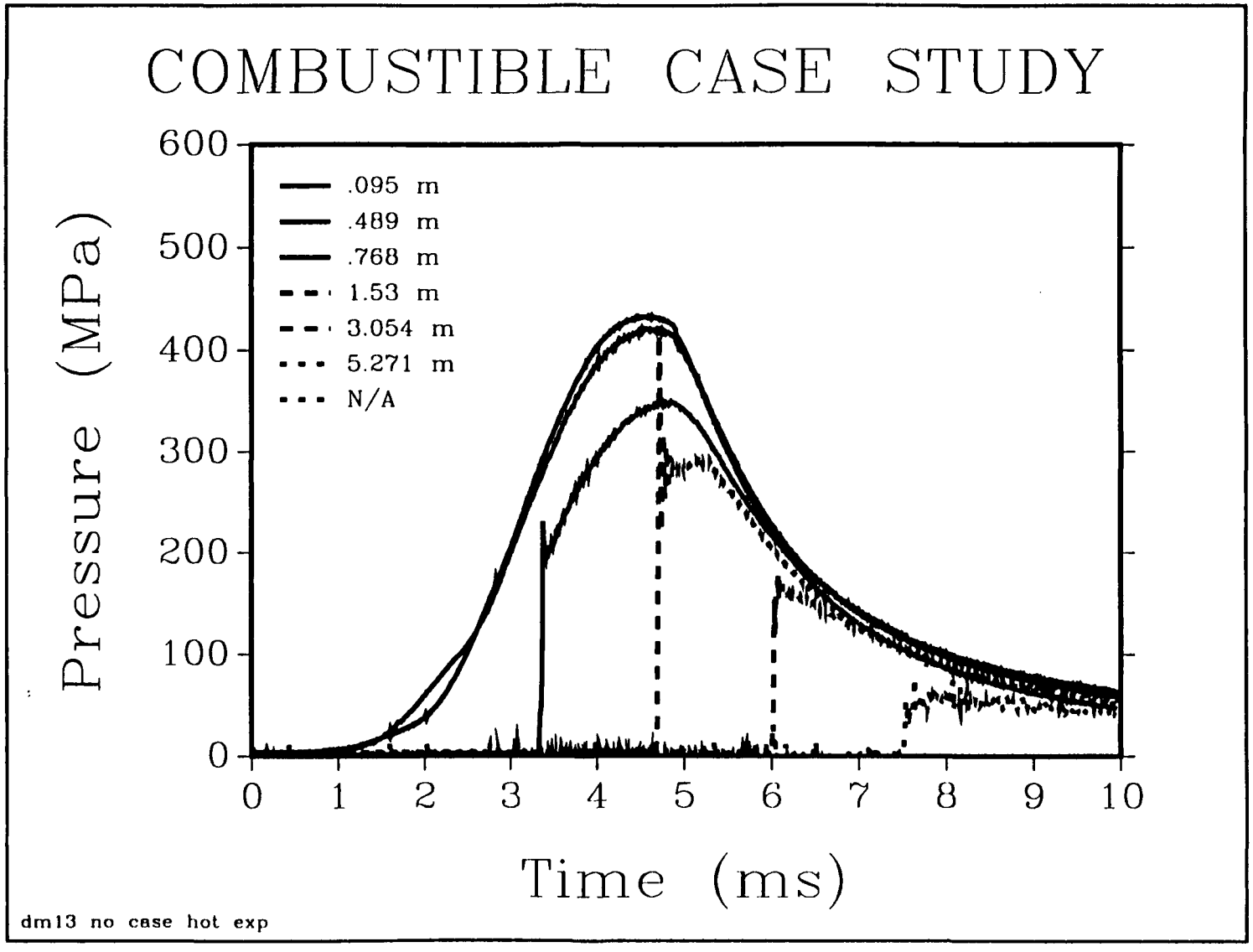


Figure 5. Experimental Pressure Time Curve - No Case - Hot.

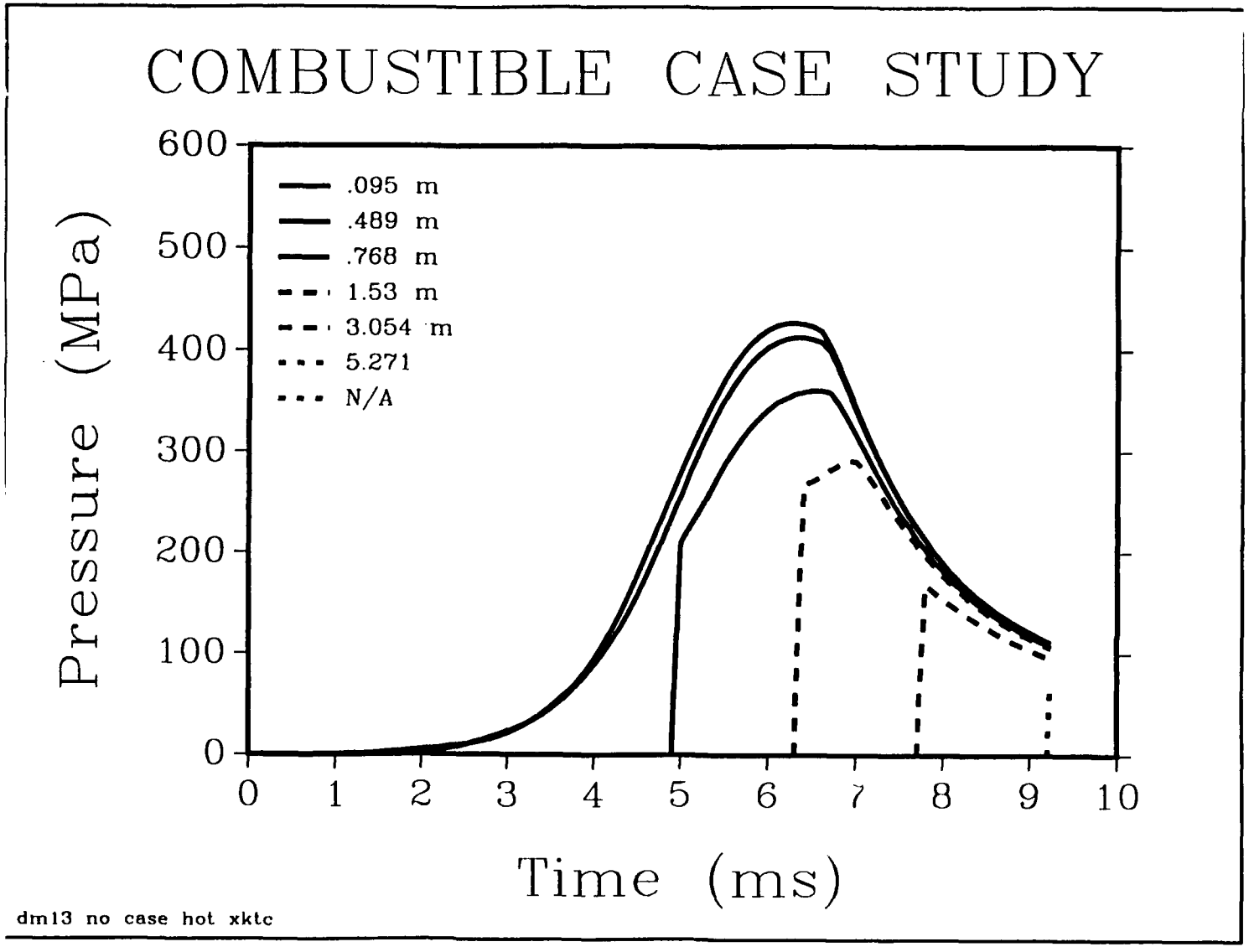


Figure 6. Theoretical Pressure Time Curve - No Case Hot.

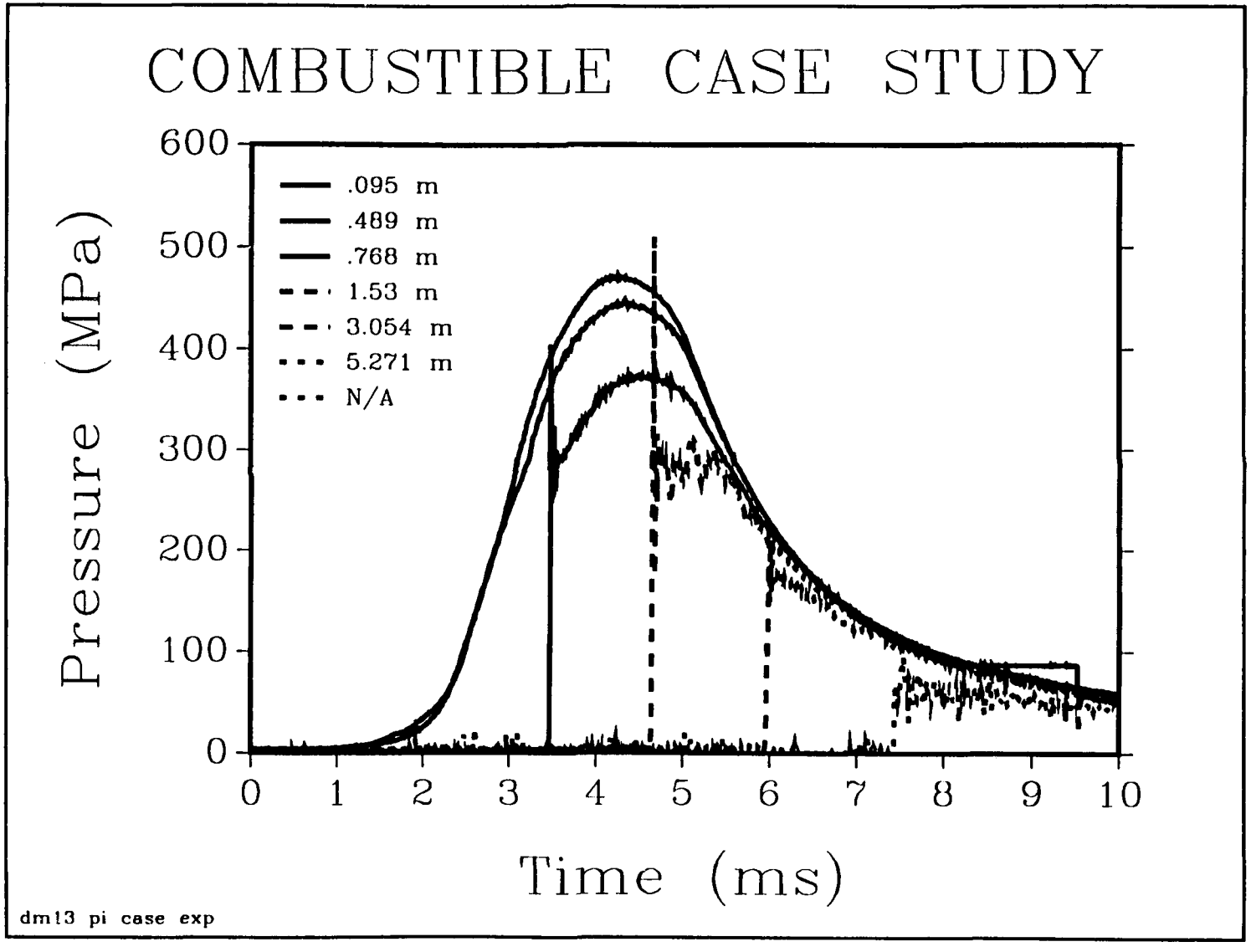


Figure 7. Experimental Pressure Time Curve - Post-Impregnated Case - Ambient.

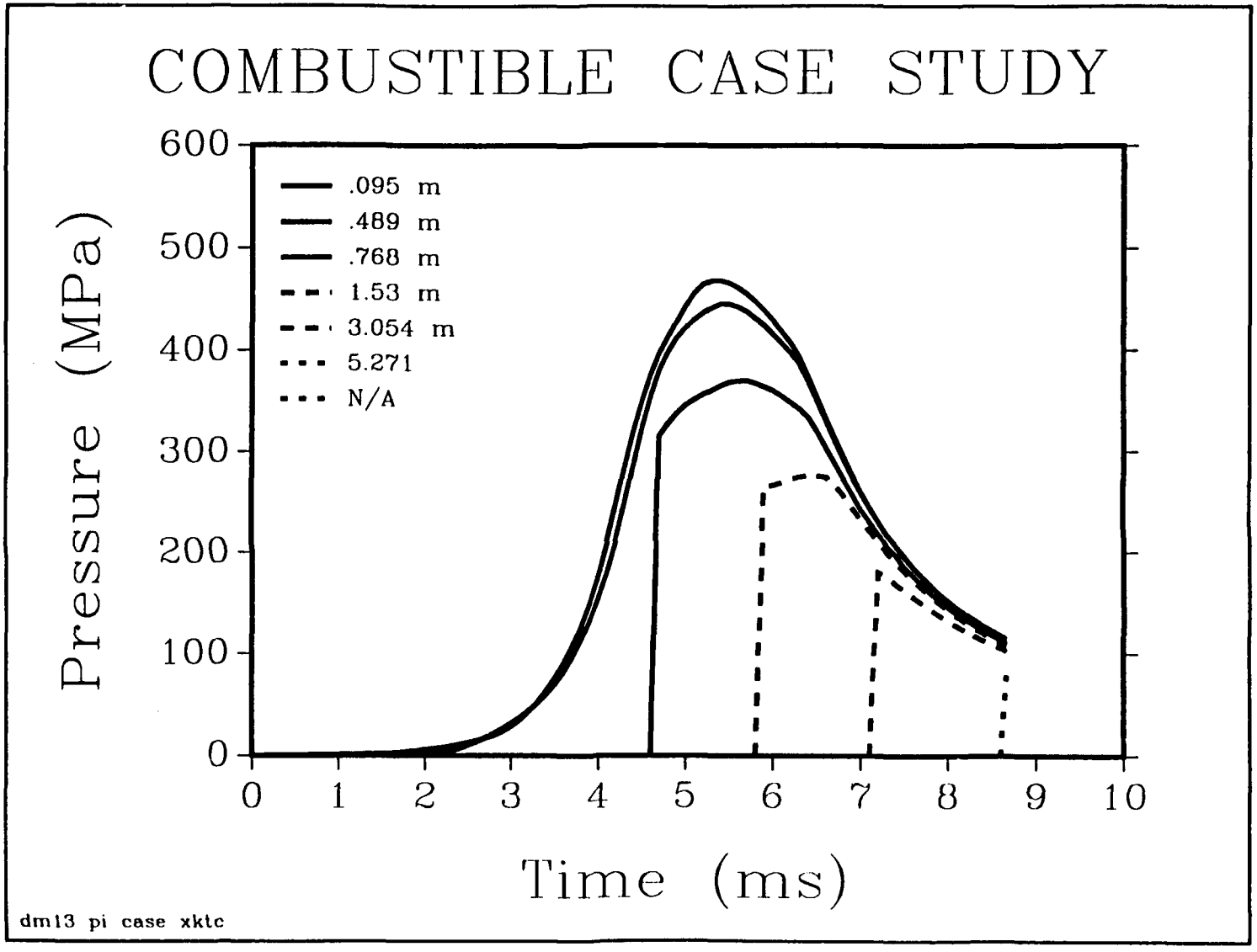


Figure 8. Theoretical Pressure Time Curve - Post-Impregnated Case - Ambient.

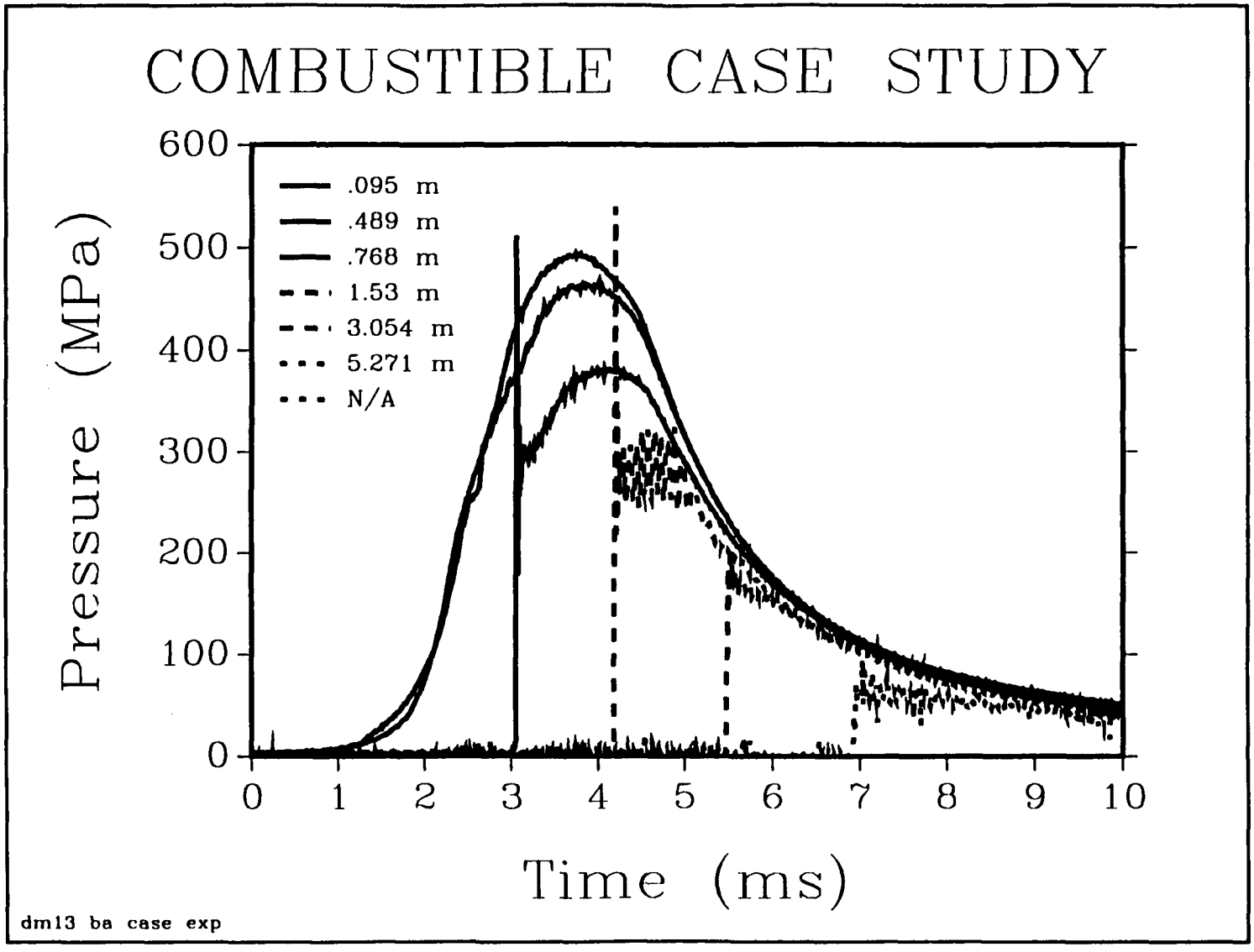


Figure 9. Experimental Pressure Time Curve - Beater Additive Case - Ambient.

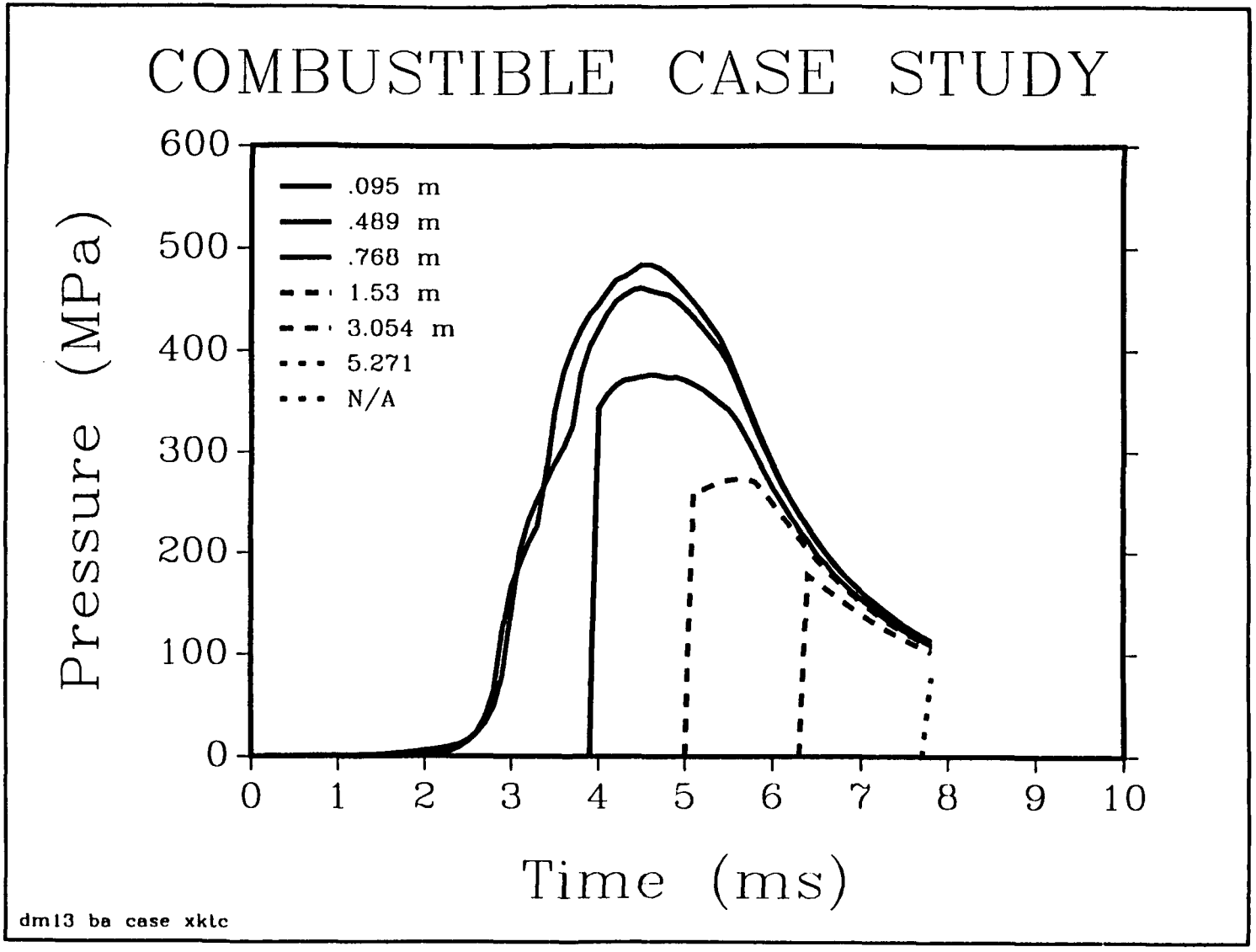


Figure 10. Theoretical Pressure Time Curve - Beater Additive Case - Ambient.

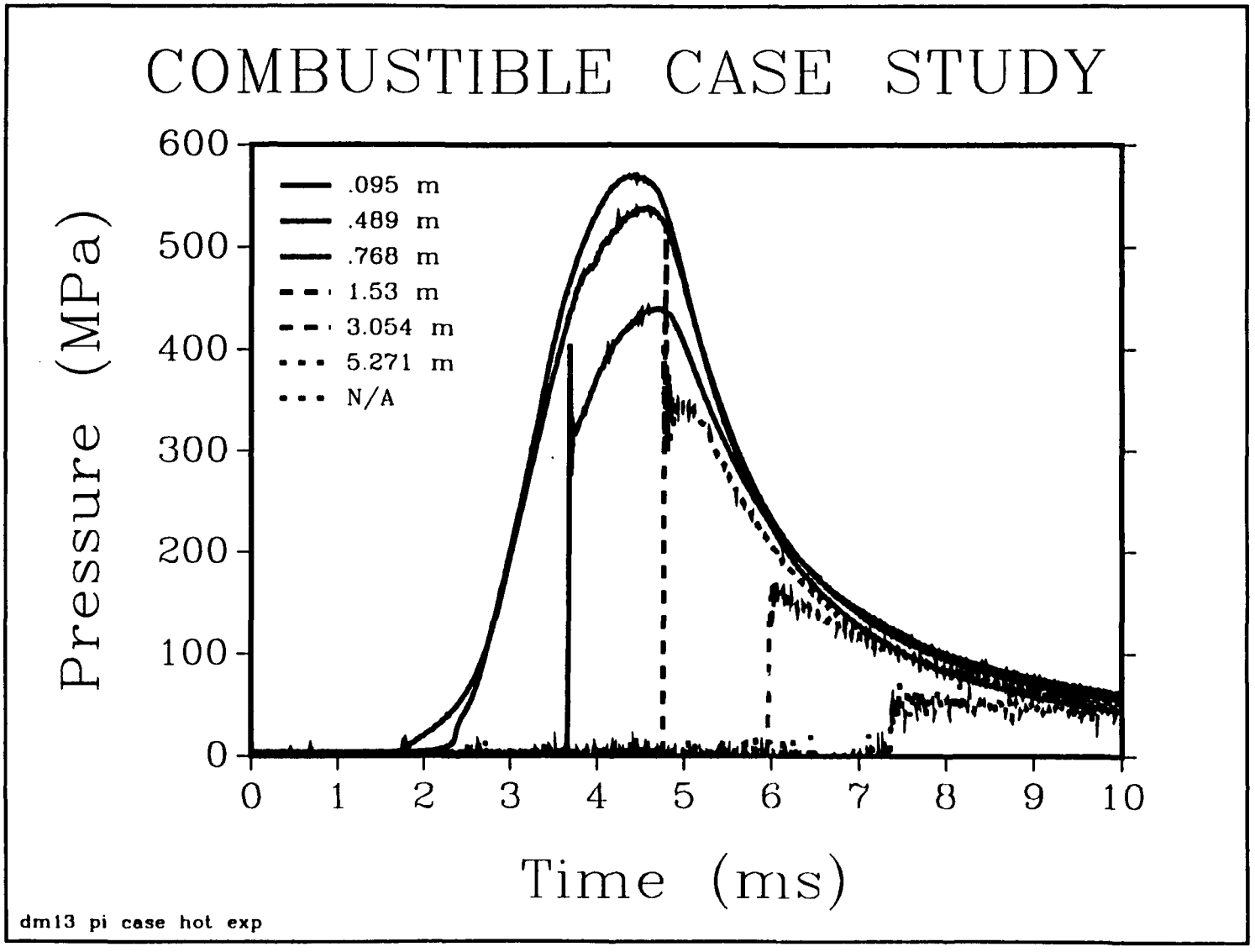


Figure 11. Experimental Pressure Time Curve - Post-Impregnated Case - Hot.

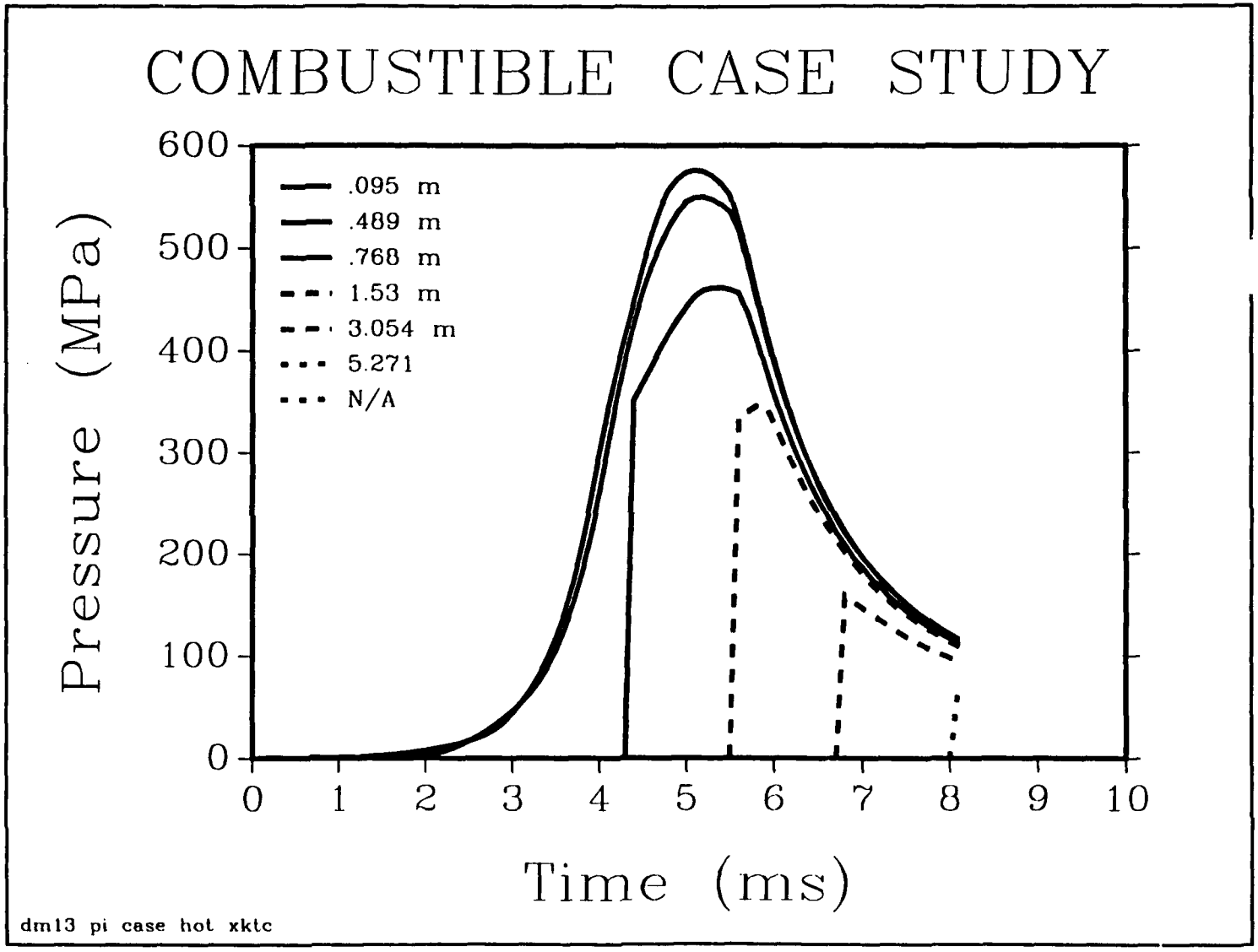


Figure 12. Theoretical Pressure Time Curve - Post-Impregnated Case - Hot.

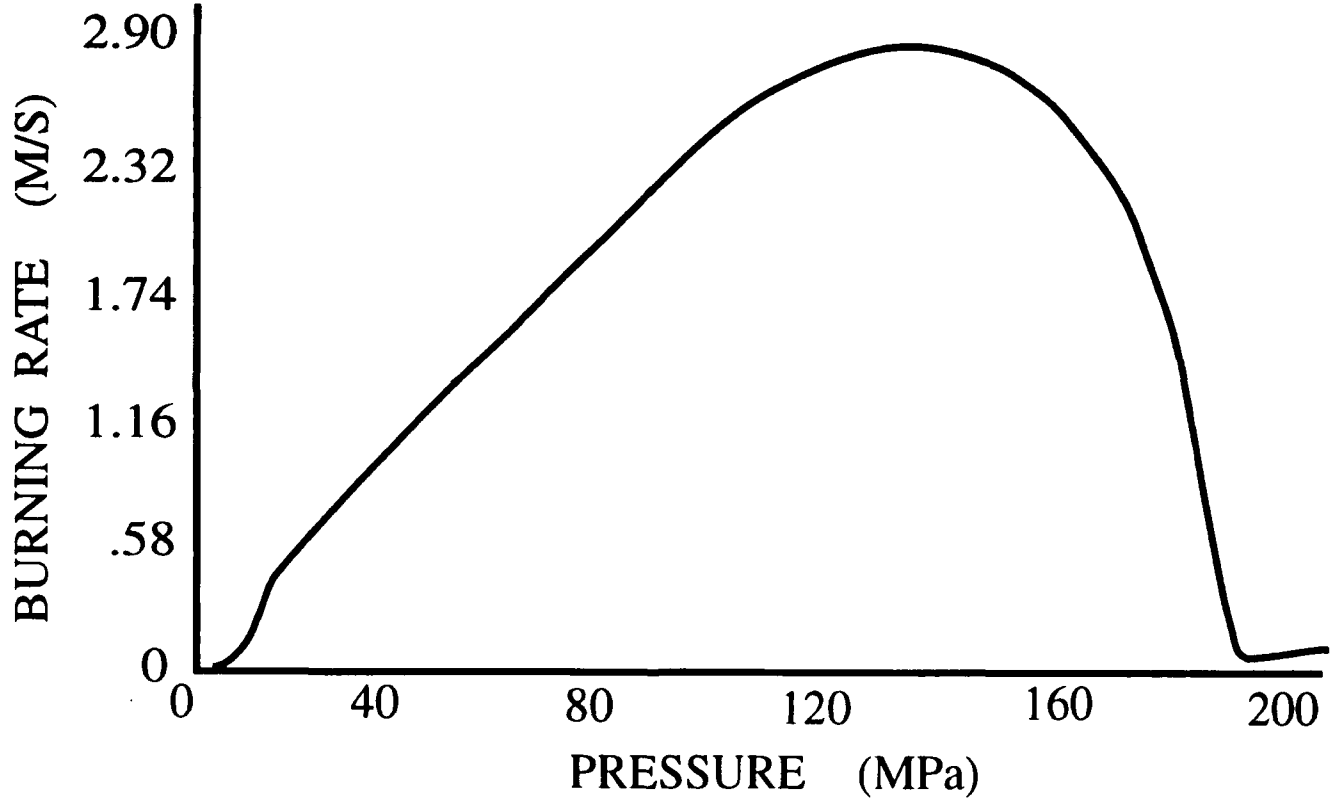


Figure 13. Burning Rate vs. Pressure of Simulated Combustible Cartridge Using the Fiber Mode.

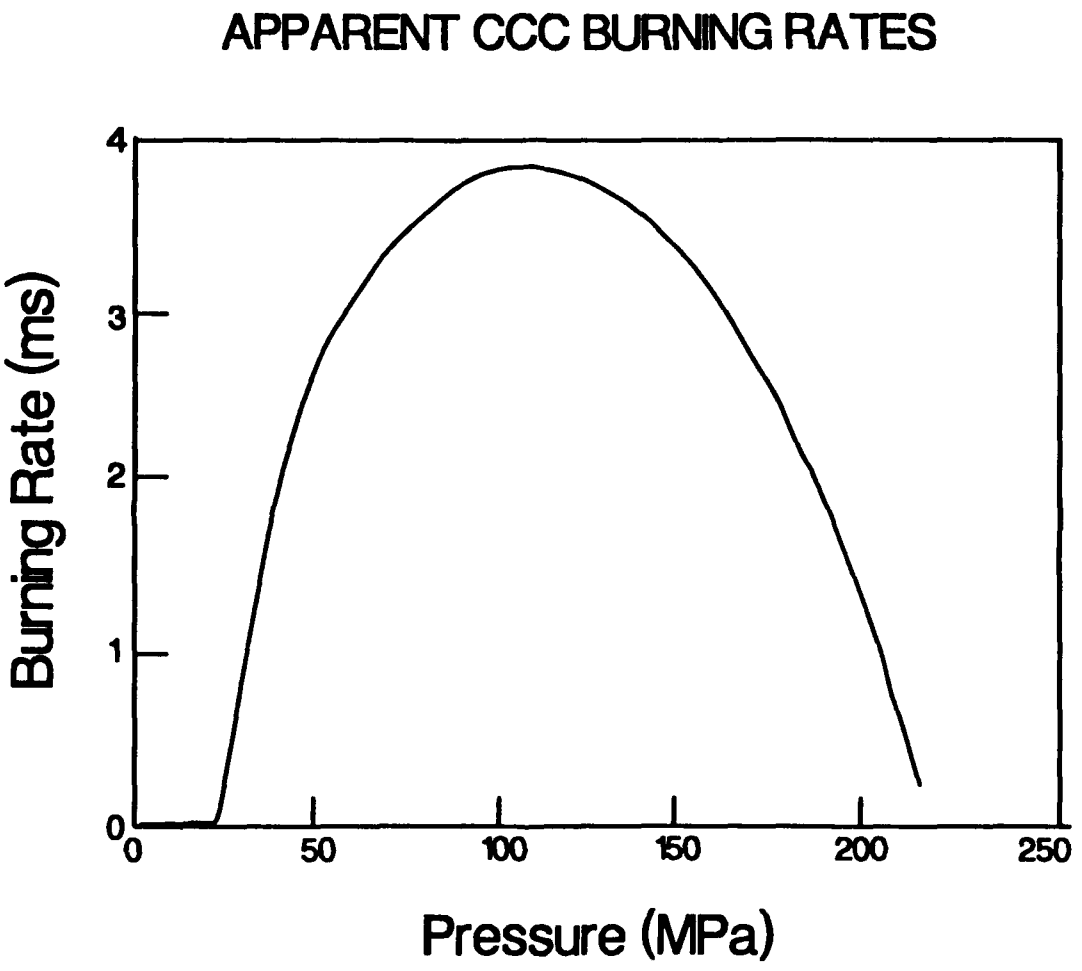


Figure 14. Burning Rate Curve for In-Depth Burning.

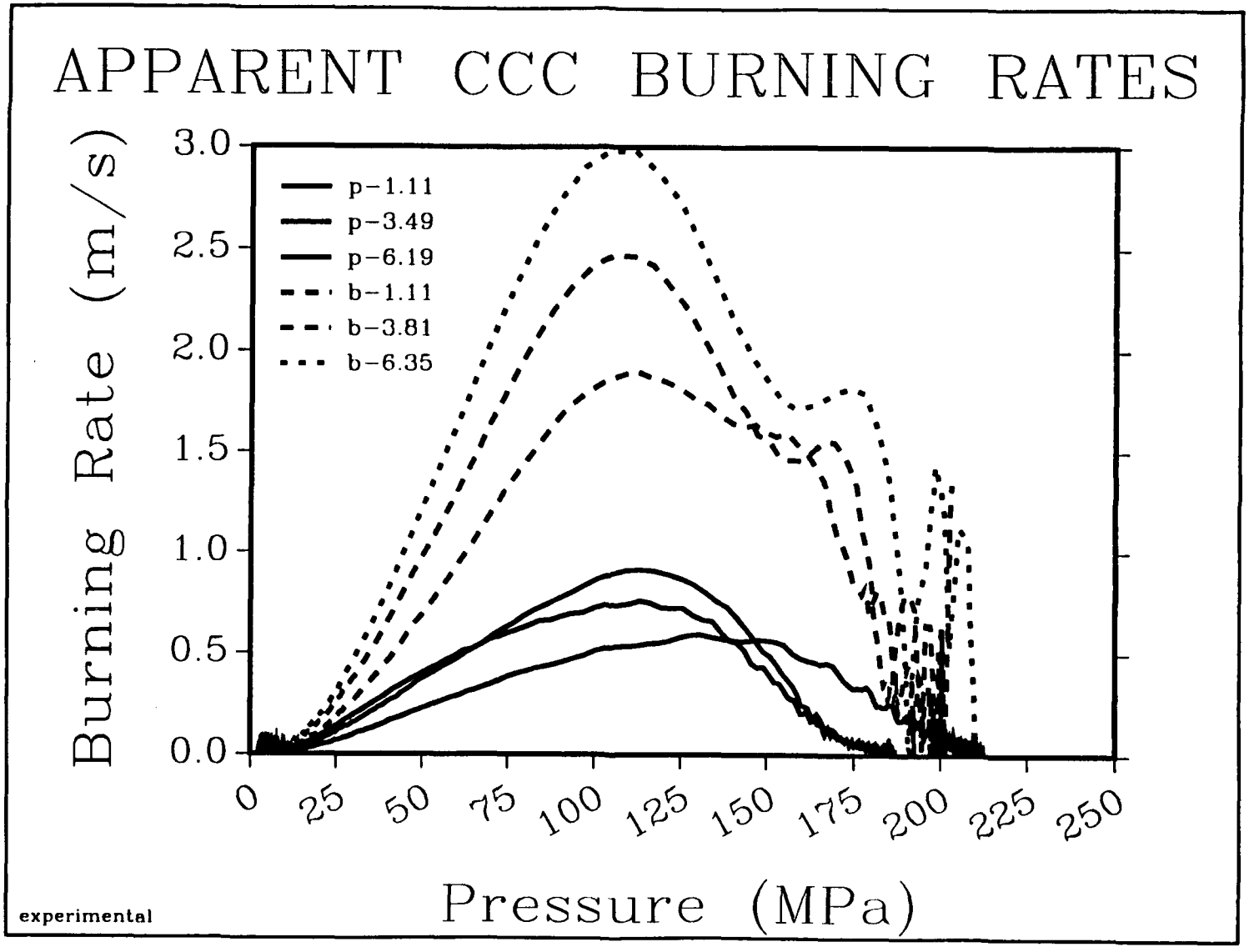


Figure 15. Apparent Burning Rates for Case Material.

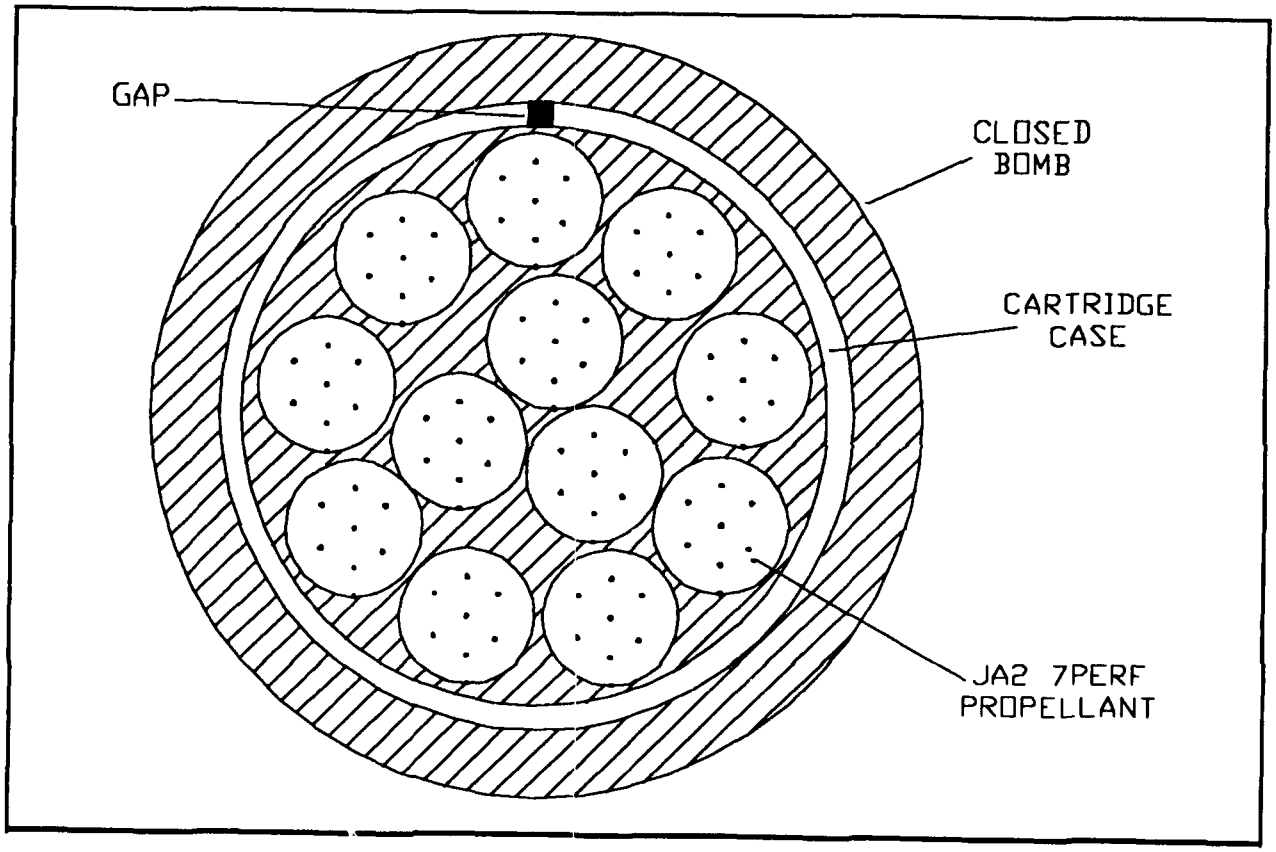


Figure 16. Interrupted Burner Configuration.

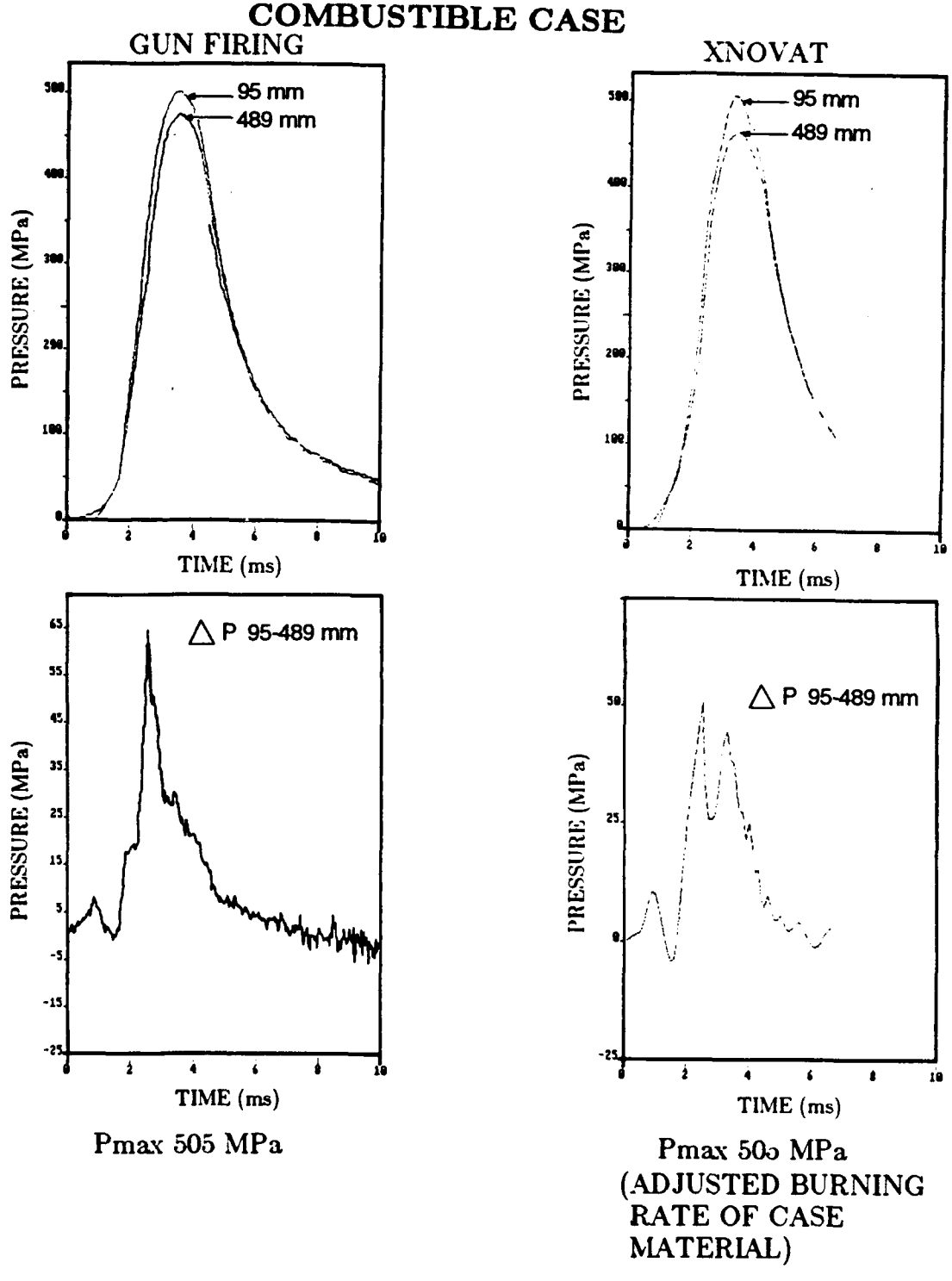


Figure 17. Calculated and Measured Pressures (a) and Pressure Differences (b) for CCC Round.

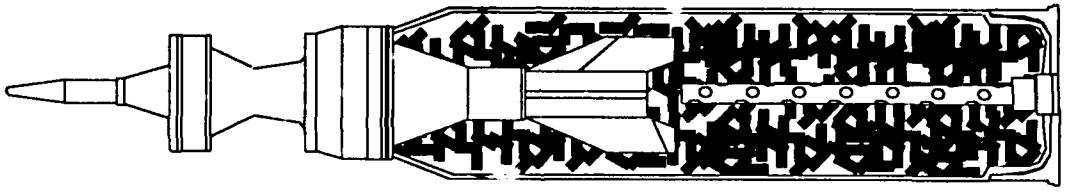

Figure 18. DM13 Line Drawing.

## 8. REFERENCES


Androutsopoulos, G. P., and R. Mann. "Evaluation of Mercury Porosimeter Experiments Using a Network Pore Structure Model." Chemical Engineering Science, vol. 34, pp. 1203–1212, 1979.

Appleman, H. C. "Combustible Ordnance in the United States." Proceedings of the 2nd Annual Australian Gun Propellant Conference, Mulwala, N.S.W., Australia. Armtec, Coachella, CA, 1986.

Brabets, R. I. "Combustible Cartridge Case Characterization." ARLCD-CR-83054, IIT Research Institute, Chicago, IL, February 1984.

Brenner, W., and M. Iqgal. "An R&D Exploratory Investigation of Resin Binders for the Combustible Cartridge Case for the 155-mm Self-Propelled (SP) Howitzer (XM198/M109A1) Ammunition." Report NYU/DAS-80-19, SBI-AD-E425 007, New York Department of Applied Sciences, New York University, October 1980.

Chirone, R., L. Massimilla, and P. Salatino. "Communication of Carbons in Fluidized Bed Combustion. Prog. Energy Combust. Sci., vol. 17, pp. 297–326, 1991.

Colburn, J. W., and F. W. Robbins. "Combustible Cartridge Case Ballistic Characterization." BRL-MR-3835, U.S. Army Ballistic Research Laboratory, Aberdeen Proving Ground, MD, May 1990.

Fisher, M. E., and J. W. Essam. "Some Cluster Size and Percolation Problem." Journal Math. Physics, vol. 2, pp. 609–619, 1961.

Gough, P. G. "The KNOVAKTC Code." BRL-CR-627, U.S. Army Ballistic Research Laboratory, Aberdeen Proving Ground, MD, February 1990.

Juhasz, A. A. (Ed.) "A Simple Closed Bomb Burning Rate Reduction Program (SIMPCB)." Round Robin Results of the Closed Bomb and Strand Burner, CPIA Publication 361, pp. IX–1–IX–30, July 1982.

Minor, T. C., and A. W. Horst. "Theoretical and Experimental Investigation of Flamespreading Processes in Combustible-Cased, Stick Propellant Charges." BRL-TR-2710, U.S. Army Ballistic Research Laboratory, Aberdeen Proving Ground, MD, February 1986.

Mohanty, K. K., J. M. Ottino, and H. T. Davis. "Reaction and Transport in Disordered Composite Media: Introduction of Percolation Concepts." Chemical Engineering Science, vol. 37, pp. 905–924, 1982.

Pfeifer, P., and D. Avnir. "Chemistry in Noninteger Dimensions Between Two and Three I. Fractal Theory of Heterogenous Surfaces." Journal Chemical Physics, vol. 79, pp. 3558–3565, 1983.

Puri, V. P. "Combustible Cartridge Cases: An Account of the Current Technology and Proposals for Future Development." WSRL-0471-TR, Weapons Systems Research Laboratory, Adelaide, Australia, October 1986.

Remaly, R. F., M. S. Nusbaum, K. G. Johnson, and S. Levive. "Duplex Combustible Cartridge Case." U.S. Patent 3 823 668, July 1974.

Robbins, F. W., and J. W. Colburn. "Modeling of the Combustible Characteristics of Combustible Cartridge Case Material." 1990 JANNAF Combustion Meeting, CPIA Publication, Warren AF Base, Cheyenne, WY, vol. 1, pp. 61–68, November 1990.

Robbins, F. W., and G. E. Keller. "Studies Supporting Development of a Modified Gradient Equation for Lumped Parameter Interior Ballistic Codes." BRL-MR-3678, U.S. Army Ballistic Research Laboratory, Aberdeen Proving Ground, MD, July 1988.

Robbins, F. W., A. A. Koszoru, and T. C. Minor. "A Theoretical and Experimental Interior Ballistic Characterization of Combustible Cases." Proceedings of the 9th International Symposium on Ballistics, ADPA, Washington, DC, April 1986.

Robbins, F. W., and D. L. Kruczynski. "Calculated Gun Interior Ballistic Effects of In-Depth Burning of VHBR Propellant." BRL-TR-3059, U.S. Army Ballistic Research Laboratory, Aberdeen Proving Ground, MD, November 1989.

Talmon, Y., and S. Prager. "Statistical Thermodynamics of Phase Equilibria in Microemulsions." Journal of Chemical Physics, vol. 69 no. 7, pp. 2984–2991.

## LIST OF SYMBOLS

| | |
|---|---|
| a | area |
| $\hat{a}$ | area [Equation (7)] |
| c | polyhedra, molar concentration |
| D | effective depth, fractal dimension, diameter |
| E | activation energy |
| $\ell$ | length |
| L | length |
| M | surface area per unit volume |
| m | mass, also mass fraction |
| r | reaction rate |
| R | radius |
| $\hat{R}$ | universal gas constraint |
| S | area |
| t | time |
| T | temperature |
| V | volume |
| x | distance |
| $\phi$ | void fraction |
| $\rho$ | density |

Subscripts

| | |
|---|---|
| a | effective |
| o | surface burning, initial |
| i | material designator |
| j | material designator |

INTENTIONALLY LEFT BLANK.

| No. of Copies | Organization |
|---|---|
| 2 | Administrator<br>Defense Technical Info Center<br>ATTN: DTIC-DDA<br>Cameron Station<br>Alexandria, VA 22304-6145 |
| 1 | Commander<br>U.S. Army Materiel Command<br>ATTN: AMCAM<br>5001 Eisenhower Ave.<br>Alexandria, VA 22333-0001 |
| 1 | Commander<br>U.S. Army Laboratory Command<br>ATTN: AMSLC-DL<br>2800 Powder Mill Rd.<br>Adelphi, MD 20783-1145 |
| 2 | Commander<br>U.S. Army Armament Research,<br>Development, and Engineering Center<br>ATTN: SMCAR-IMI-I<br>Picatinny Arsenal, NJ 07806-5000 |
| 2 | Commander<br>U.S. Army Armament Research,<br>Development, and Engineering Center<br>ATTN: SMCAR-TDC<br>Picatinny Arsenal, NJ 07806-5000 |
| 1 | Director<br>Benet Weapons Laboratory<br>U.S. Army Armament Research,<br>Development, and Engineering Center<br>ATTN: SMCAR-CCB-TL<br>Watervliet, NY 12189-4050 |
| (Unclass. only) 1 | Commander<br>U.S. Army Rock Island Arsenal<br>ATTN: SMCRI-TL/Technical Library<br>Rock Island, IL 61299-5000 |
| 1 | Director<br>U.S. Army Aviation Research<br>and Technology Activity<br>ATTN: SAVRT-R (Library)<br>M/S 219-3<br>Ames Research Center<br>Moffett Field, CA 94035-1000 |
| 1 | Commander<br>U.S. Army Missile Command<br>ATTN: AMSMI-RD-CS-R (DOC)<br>Redstone Arsenal, AL 35898-5010 |

| No. of Copies | Organization |
|---|---|
| 1 | Commander<br>U.S. Army Tank-Automotive Command<br>ATTN: ASQNC-TAC-DIT (Technical<br>Information Center)<br>Warren, MI 48397-5000 |
| 1 | Director<br>U.S. Army TRADOC Analysis Command<br>ATTN: ATRC-WSR<br>White Sands Missile Range, NM 88002-5502 |
| 1 | Commandant<br>U.S. Army Field Artillery School<br>ATTN: ATSF-CSI<br>Ft. Sill, OK 73503-5000 |
| (Class. only) 1 | Commandant<br>U.S. Army Infantry School<br>ATTN: ATSH-CD (Security Mgr.)<br>Fort Benning, GA 31905-5660 |
| (Unclass. only) 1 | Commandant<br>U.S. Army Infantry School<br>ATTN: ATSH-CD-CSO-OR<br>Fort Benning, GA 31905-5660 |
| 1 | WL/MNOI<br>Eglin AFB, FL 32542-5000 |
| | Aberdeen Proving Ground |
| 2 | Dir, USAMSAA<br>ATTN: AMXSY-D<br>AMXSY-MP, H. Cohen |
| 1 | Cdr, USATECOM<br>ATTN: AMSTE-TC |
| 3 | Cdr, CRDEC, AMCCOM<br>ATTN: SMCCR-RSP-A<br>SMCCR-MU<br>SMCCR-MSI |
| 1 | Dir, VLAMO<br>ATTN: AMSLC-VL-D |
| 10 | Dir, USABRL<br>ATTN: SLCBR-DD-T |

| No. of Copies | Organization |
|---|---|
| 1 | Commander<br>U.S. Army Concepts Analysis Agency<br>ATTN: D. Hardison<br>8120 Woodmont Ave.<br>Bethesda, MD 20014 |
| 1 | C.I.A.<br>01R/DB/Standard<br>Washington, DC 20505 |
| 1 | Director<br>U.S. Army Ballistic Missile<br>Defense Systems Command<br>Advanced Technology Center<br>P. O. Box 1500<br>Huntsville, AL 35807-3801 |
| 1 | Chairman<br>DOD Explosives Safety Board<br>Room 856-C<br>Hoffman Bldg. 1<br>2461 Eisenhower Ave.<br>Alexandria, VA 22331-0600 |
| 1 | Department of the Army<br>Office of the Product Manager<br>155mm Howitzer, M109A6, Paladin<br>ATTN: SFAE-AR-HIP-IP, Mr. R. De Kleine<br>Picatinny Arsenal, NJ 07806-5000 |
| 2 | Commander<br>Production Base Modernization Agency<br>U.S. Army Armament Research,<br>Development, and Engineering Center<br>ATTN: AMSMC-PBM, A. Siklosi<br>AMSMC-PBM-E, L. Laibson<br>Picatinny Arsenal, NJ 07806-5000 |
| 3 | PEO-Armaments<br>Project Manager<br>Tank Main Armament Systems<br>ATTN: AMCPM-TMA/K. Russell<br>AMCPM-TMA-105<br>AMCPM-TMA-120, C. Roller<br>Picatinny Arsenal, NJ 07806-5000 |

| No. of Copies | Organization |
|---|---|
| 15 | Commander<br>U.S. Army Armament Research,<br>Development, and Engineering Center<br>ATTN: SMCAR-AEE<br>SMCAR-AEE-B,<br>A. Beardell<br>D. Downs<br>S. Einstein<br>S. Westley<br>S. Bernstein<br>J. Rutkowski<br>B. Brodman<br>R. Cirincione<br>A. Grabowsky<br>P. Hui<br>J. O'Reilly<br>P. O'Reilly<br>N. DeVries<br>SMCAR-AES, S. Kaplowitz, Bldg. 321<br>Picatinny Arsenal, NJ 07806-5000 |
| 2 | Commander<br>U.S. Army Armament Research,<br>Development, and Engineering Center<br>ATTN: SMCAR-CCD, D. Spring<br>SMCAR-CCH-V, C. Mandala<br>Picatinny Arsenal, NJ 07806-5000 |
| 1 | Commander<br>U.S. Army Armament Research,<br>Development, and Engineering Center<br>ATTN: SMCAR-HFM, E. Barrieres<br>Picatinny Arsenal, NJ 07806-5000 |
| 1 | Commander<br>U.S. Army Armament Research,<br>Development, and Engineering Center<br>ATTN: SMCAR-FSA-T, M. Salsbury<br>Picatinny Arsenal, NJ 07806-5000 |
| 1 | Commander, USACECOM<br>R&D Technical Library<br>ATTN: ASQNC-ELC-IS-L-R, Myer Center<br>Fort Monmouth, NJ 07703-5301 |

| No. of Copies | Organization |
|---|---|
| 1 | Commander<br>U.S. Army Harry Diamond Laboratories<br>ATTN: SLCHD-TA-L<br>2800 Powder Mill Rd.<br>Adelphi, MD 20783-1145 |
| 1 | Commandant<br>U.S. Army Aviation School<br>ATTN: Aviation Agency<br>Fort Rucker, AL 36360 |
| 2 | Program Manager<br>U.S. Army Tank-Automotive Command<br>ATTN: AMCPM-ABMS, T. Dean (2 cps)<br>Warren, MI 48092-2498 |
| 1 | Program Manager<br>U.S. Army Tank-Automotive Command<br>Fighting Vehicles Systems<br>ATTN: SFAE-ASM-BV<br>Warren, MI 48092-2498 |
| 1 | Project Manager<br>Abrams Tank System<br>ATTN: SFAE-ASM-AB<br>Warren, MI 48397-5000 |
| 1 | Director<br>HQ, TRAC RPD<br>ATTN: ATCD-MA<br>Fort Monroe, VA 23651-5143 |
| 2 | Director<br>U.S. Army Materials Technology Laboratory<br>ATTN: SLCMT-ATL (2 cps)<br>Watertown, MA 02172-0001 |
| 1 | Commander<br>U.S. Army Research Office<br>ATTN: Technical Library<br>P.O. Box 12211<br>Research Triangle Park, NC 27709-2211 |
| 1 | Commander<br>U.S. Army Belvoir Research and Development Center<br>ATTN: STRBE-WC<br>Fort Belvoir, VA 22060-5006 |

| No. of Copies | Organization |
|---|---|
| 1 | Director<br>U.S. Army TRAC-Ft. Lee<br>ATTN: ATRC-L, Mr. Cameron<br>Fort Lee, VA 23801-6140 |
| 1 | Commandant<br>U.S. Army Command and General Staff College<br>Fort Leavenworth, KS 66027 |
| 1 | Commandant<br>U.S. Army Special Warfare School<br>ATTN: Rev and Trng Lit Div<br>Fort Bragg, NC 28307 |
| 3 | Commander<br>Radford Army Ammunition Plant<br>ATTN: SMCAR-QA/HI LIB (3 cps)<br>Radford, VA 24141-0298 |
| 1 | Commander<br>U.S. Army Foreign Science and Technology Center<br>ATTN: AMXST-MC-3<br>220 Seventh Street, NE<br>Charlottesville, VA 22901-5396 |
| 2 | Commander<br>Naval Sea Systems Command<br>ATTN: SEA 62R<br>SEA 64<br>Washington, DC 20362-5101 |
| 1 | Commander<br>Naval Air Systems Command<br>ATTN: AIR-954-Technical Library<br>Washington, DC 20360 |
| 1 | Naval Research Laboratory<br>Technical Library<br>Washington, DC 20375 |
| 2 | Commandant<br>U.S. Army Field Artillery Center and School<br>ATTN: ATSF-CO-MW, E. Dublisky (2 cps)<br>Fort Sill, OK 73503-5600 |

| No. of Copies | Organization |
|---|---|
| 1 | Office of Naval Research<br>ATTN: Code 473, R. S. Miller<br>800 N. Quincy Street<br>Arlington, VA 22217-9999 |
| 3 | Commandant<br>U.S. Army Armor School<br>ATTN: ATZK-CD-MS, M. Falkovitch (3 cps)<br>Armor Agency<br>Fort Knox, KY 40121-5215 |
| 2 | Commander<br>U.S. Naval Surface Warfare Center<br>ATTN: J. P. Consaga<br>C. Gotzmer<br>Indian Head, MD 20640-5000 |
| 4 | Commander<br>Naval Surface Warfare Center<br>ATTN: Code 730<br>Code R-13,<br>K. Kim<br>R. Bernecker<br>H. Sandusky<br>Silver Spring, MD 20903-5000 |
| 2 | Commanding Officer<br>Naval Underwater Systems Center<br>ATTN: Code 5B331, R. S. Lazar<br>Technical Library<br>Newport, RI 02840 |
| 1 | Director<br>Benet Weapons Laboratories<br>ATTN: SMCAR-CCB-RA, G. P. O'Hara<br>Watervliet, NY 12189-4050 |
| 4 | Commander<br>Dahlgren Division<br>Naval Surface Warfare Center<br>ATTN: Code G30, Guns and Munitions Division<br>Code G301, D. Wilson<br>Code G32, Gun Systems Branch<br>Code E23, Technical Library<br>Dahlgren, VA 22448-5000 |

| No. of Copies | Organization |
|---|---|
| 3 | Commander<br>Naval Weapons Center<br>ATTN: Code 388, C. F. Price<br>Code 3895, T. Parr<br>Information Science Division<br>China Lake, CA 93555-6001 |
| 1 | OSD/SDIO/IST<br>ATTN: Dr. Len Caveny<br>Pentagon<br>Washington, DC 20301-7100 |
| 4 | Commander<br>Indian Head Division<br>Naval Surface Warfare Center<br>ATTN: Code 610, T. C. Smith<br>D. Brooks<br>K. Rice<br>Technical Library<br>Indian Head, MD 20640-5035 |
| 1 | OLAC PL/TSTL<br>ATTN: D. Shiplett<br>Edwards AFB, CA 93523-5000 |
| 1 | AFATL/DLYV<br>Eglin AFB, FL 32542-5000 |
| 1 | AFATL/DLXP<br>Eglin AFB, FL 32542-5000 |
| 1 | AFATL/DLJE<br>Eglin AFB, FL 32542-5000 |
| 1 | AFELM, The Rand Corporation<br>ATTN: Library D<br>1700 Main Street<br>Santa Monica, CA 90401-3297 |
| 3 | AAI Corporation<br>ATTN: J. Hebert<br>J. Frankle<br>D. Cleveland<br>P.O. Box 126<br>Hunt Valley, MD 21030-0126 |

| No. of Copies | Organization |
|---|---|
| 3 | AL/LSCF<br>ATTN: J. Levine<br>L. Quinn<br>T. Edwards<br>Edwards AFB, CA 93523-5000 |
| 1 | AVCO Everett Research Laboratory<br>ATTN: D. Stickler<br>2385 Revere Beach Parkway<br>Everett, MA 02149-5936 |
| 1 | General Electric Company<br>Tactical Systems Department<br>ATTN: J. Mandzy<br>100 Plastics Ave.<br>Pittsfield, MA 01201-3698 |
| 1 | IITRI<br>ATTN: M. J. Klein<br>10 W. 35th Street<br>Chicago, IL 60616-3799 |
| 1 | Hercules, Inc.<br>Allegheny Ballistics Laboratory<br>ATTN: William B. Walkup<br>P.O. Box 210<br>Rocket Center, WV 26726 |
| 1 | Hercules, Inc.<br>Radford Army Ammunition Plant<br>ATTN: E. Hibshman<br>Radford, VA 24141-0299 |
| 1 | Hercules, Inc.<br>Hercules Plaza<br>ATTN: B. M. Riggleman<br>Wilmington, DE 19894 |
| 3 | Director<br>Lawrence Livermore National Laboratory<br>ATTN: L-355,<br>A. Buckingham<br>M. Finger<br>L-324, M. Constantino<br>P.O. Box 808<br>Livermore, CA 94550-0622 |

| No. of Copies | Organization |
|---|---|
| 1 | Olin Corporation<br>Badger Army Ammunition Plant<br>ATTN: F. E. Wolf<br>Baraboo, WI 53913 |
| 3 | Olin Ordnance<br>ATTN: E. J. Kirschke<br>A. F. Gonzalez<br>D. W. Worthington<br>P.O. Box 222<br>St. Marks, FL 32355-0222 |
| 1 | Olin Ordnance<br>ATTN: H. A. McElroy<br>10101 9th Street, North<br>St. Petersburg, FL 33716 |
| 1 | Paul Gough Associates, Inc.<br>ATTN: Dr. Paul S. Gough<br>1048 South Street<br>Portsmouth, NH 03801-5423 |
| 1 | Physics International Company<br>ATTN: Library, H. Wayne Wampler<br>2700 Merced Street<br>San Leandro, CA 98457-5602 |
| 1 | Princeton Combustion Research Laboratory, Inc.<br>ATTN: M. Summerfield<br>475 U.S. Highway One<br>Monmouth Junction, NJ 08852-9650 |
| 2 | Rockwell International<br>Rocketdyne Division<br>ATTN: BA08,<br>J.E. Flanagan<br>J. Gray<br>6633 Canoga Ave.<br>Canoga Park, CA 91303-2703 |
| 1 | Sverdrup Technology, Inc.<br>ATTN: Dr. John Deur<br>2001 Aerospace Parkway<br>Brook Park, OH 44142 |

| No. of Copies | Organization |
|---|---|
| 2 | Thiokol Corporation<br>Elkton Division<br>ATTN: R. Biddle<br>Technical Library<br>P.O. Box 241<br>Elkton, MD 21921-0241 |
| 1 | Veritay Technology, Inc.<br>ATTN: E. Fisher<br>4845 Millersport Highway<br>East Amherst, NY 14501-0305 |
| 1 | Universal Propulsion Company<br>ATTN: H. J. McSpadden<br>25401 North Central Ave.<br>Phoenix, AZ 85027-7837 |
| 1 | Battelle<br>ATTN: TACTEC Library, J.N. Huggins<br>505 King Ave.<br>Columbus, OH 43201-2693 |
| 1 | Brigham Young University<br>Department of Chemical Engineering<br>ATTN: M. Beckstead<br>Provo, UT 84601 |
| 1 | California Institute of Technology<br>204 Karman Laboratory<br>Main Stop 301-46<br>ATTN: F.E.C. Culick<br>1201 E. California Street<br>Pasadena, CA 91109 |
| 1 | Jet Propulsion Laboratory<br>California Institute of Technology<br>ATTN: L. Strand, MS 125-224<br>4800 Oak Grove Drive<br>Pasadena, CA 91109-8099 |
| 1 | University of Illinois<br>Department of Mechanical/Industrial Engineering<br>ATTN: H. Krier<br>144 MEB; 1206 N. Green Street<br>Urbana, IL 61801-2978 |

| No. of Copies | Organization |
|---|---|
| 1 | University of Massachusetts<br>Department of Mechanical Engineering<br>ATTN: K. Jakus<br>Amherst, MA 01002-0014 |
| 1 | University of Minnesota<br>Department of Mechanical Engineering<br>ATTN: E. Fletcher<br>Minneapolis, MN 55414-3368 |
| 3 | Georgia Institute of Technology<br>School of Aerospace Engineering<br>ATTN: B.T. Zim<br>E. Price<br>W.C. Strahle<br>Atlanta, GA 30332 |
| 1 | Institute of Gas Technology<br>ATTN: D. Gidaspow<br>3424 S. State Street<br>Chicago, IL 60616-3896 |
| 1 | Johns Hopkins University<br>Applied Physics Laboratory<br>Chemical Propulsion<br>Information Agency<br>ATTN: T. Christian<br>Johns Hopkins Road<br>Laurel, MD 20707-0690 |
| 1 | Massachusetts Institute of Technology<br>Department of Mechanical Engineering<br>ATTN: T. Toong<br>77 Massachusetts Ave.<br>Cambridge, MA 02139-4307 |
| 1 | Pennsylvania State University<br>Department of Mechanical Engineering<br>ATTN: V. Yang<br>University Park, PA 16802-7501 |
| 1 | Pennsylvania State University<br>Department of Mechanical Engineering<br>ATTN: K. Kuo<br>University Park, PA 16802-7501 |

| No. of Copies | Organization |
|---|---|
| 1 | Pennsylvania State University<br>Assistant Professor<br>Department of Mechanical Engineering<br>ATTN: Dr. Stefan T. Thynell<br>219 Hallowell Building<br>University Park, PA 16802-7501 |
| 1 | Pennsylvania State University<br>Director, Gas Dynamics Laboratory<br>Department of Mechanical Engineering<br>ATTN: Dr. Gary S. Settles<br>303 Mechanical Engineering Building<br>University Park, PA 16802-7501 |
| 1 | SRI International<br>Propulsion Sciences Division<br>ATTN: Technical Library<br>333 Ravenwood Ave.<br>Menlo Park, CA 94025-3493 |
| 1 | Rensselaer Polytechnic Institute<br>Department of Mathematics<br>Troy, NY 12181 |
| 2 | Director<br>Los Alamos Scientific Laboratory<br>ATTN: T3, D. Butler<br>M. Division, B. Craig<br>P.O. Box 1663<br>Los Alamos, NM 87544 |
| 1 | General Applied Sciences Laboratory<br>ATTN: J. Erdos<br>77 Raynor Ave.<br>Ronkonkama, NY 11779-6649 |
| 1 | Battelle PNL<br>ATTN: Mr. Mark Garnich<br>P.O. Box 999<br>Richland, WA 99352 |
| 1 | Stevens Institute of Technology<br>Davidson Laboratory<br>ATTN: R. McAlevy III<br>Castle Point Station<br>Hoboken, NJ 07030-5907 |

| No. of Copies | Organization |
|---|---|
| 1 | Rutgers University<br>Department of Mechanical and Aerospace Engineering<br>ATTN: S. Temkin<br>University Heights Campus<br>New Brunswick, NJ 08903 |
| 1 | University of Southern California<br>Mechanical Engineering Department<br>ATTN: 0HE200, M. Gerstein<br>Los Angeles, CA 90089-5199 |
| 1 | University of Utah<br>Department of Chemical Engineering<br>ATTN: A. Baer<br>Salt Lake City, UT 84112-1194 |
| 1 | Washington State University<br>Department of Mechanical Engineering<br>ATTN: C. T. Crowe<br>Pullman, WA 99163-5201 |
| 1 | Alliant Techsystems, Inc.<br>ATTN: R. E. Tompkins<br>*MN38-3300*<br>5700 Smetana Drive<br>Minnetonka, MN 55343 |
| 1 | Alliant Techsystems, Inc.<br>ATTN: J. Kennedy<br>7225 Northland Drive<br>Brooklyn Park, MN 55428 |
| 1 | Science Applications, Inc.<br>ATTN: R. B. Edelman<br>23146 Cumorah Crest Drive<br>Woodland Hills, CA 91364-3710 |
| 1 | Battelle Columbus Laboratories<br>ATTN: Mr. Victor Levin<br>505 King Ave.<br>Columbus, OH 43201-2693 |
| 1 | Allegheny Ballistics Laboratory<br>Propulsion Technology Department<br>Hercules Aerospace Company<br>ATTN: Mr. Thomas F. Farabaugh<br>P.O. Box 210<br>Rocket Center, WV 26726 |

| No. of Copies | Organization |
|---|---|
| 1 | MBR Research Inc.<br>ATTN: Dr. Moshe Ben-Reuven<br>601 Ewing St., Suite C-22<br>Princeton, NJ 08540 |
| | Aberdeen Proving Ground |
| 1 | Cdr, USACSTA<br>ATTN: STECS-PO, R. Hendricksen |

## USER EVALUATION SHEET/CHANGE OF ADDRESS

This Laboratory undertakes a continuing effort to improve the quality of the reports it publishes. Your comments/answers to the items/questions below will aid us in our efforts.

1. BRL Report Number BRL-TR-3383 Date of Report August 1992

2. Date Report Received _____

3. Does this report satisfy a need? (Comment on purpose, related project, or other area of interest for which the report will be used.) _____

4. Specifically, how is the report being used? (Information source, design data, procedure, source of ideas, etc.) _____

5. Has the information in this report led to any quantitative savings as far as man-hours or dollars saved, operating costs avoided, or efficiencies achieved, etc? If so, please elaborate. _____

6. General Comments. What do you think should be changed to improve future reports? (Indicate changes to organization, technical content, format, etc.) _____

CURRENT ADDRESS

_____
Name

_____
Organization

_____
Address

_____
City, State, Zip Code

7. If indicating a Change of Address or Address Correction, please provide the New or Correct Address in Block 6 above and the Old or Incorrect address below.

OLD ADDRESS

_____
Name

_____
Organization

_____
Address

_____
City, State, Zip Code

(Remove this sheet, fold as indicated, staple or tape closed, and mail.)

DEPARTMENT OF THE ARMY
Director
U.S. Army Ballistic Research Laboratory
ATTN: SLCBR-DD-T
Aberdeen Proving Ground, MD 21005-5066

OFFICIAL BUSINESS

**BUSINESS REPLY MAIL**
FIRST CLASS PERMIT No 0001, APG, MD

Postage will be paid by addressee.

Director
U.S. Army Ballistic Research Laboratory
ATTN: SLCBR-DD-T
Aberdeen Proving Ground, MD 21005-5066

NO POSTAGE
NECESSARY
IF MAILED
IN THE
UNITED STATES